Nitrate and nitrite reduction by ferrous iron minerals in polluted groundwater: Isotopic characterization of batch experiments.

Rosanna Margalef-Marti, Raúl Carrey, José Antonio Benito, Vicenç Marti, Albert Soler, Neus Otero

Chemical Geology, 2020
DOI: https://doi.org/10.1016/j.chemgeo.2020.119691

Received date: 23 January 2020
Revised date: 20 May 2020
Accepted date: 21 May 2020
Available online: 25 May 2020

Nitrate and nitrite reduction by ferrous iron minerals in polluted groundwater: Isotopic characterization of batch experiments

Rosanna Margalef-Marti[1,2], Raúl Carrey[1,2], José Antonio Benito[3], Vicenç Marti[3], Albert Soler[1,2], Neus Otero[1,2,4]

[1] Grup MAiMA, SGR Mineralogia Aplicada, Geoquímica i Geomicrobiologia, SIMGEO UB-CSIC, Departament de Mineralogia, Petrologia i Geologia Aplicada, Facultat de Ciències de la Terra, Universitat de Barcelona (UB), C/Martí i Franquès s/n, 08028 Barcelona (Spain).

[2] Institut de Recerca de l'Aigua (IdRA), UB, 08001 Barcelona (Spain).

[3] Materials Science and Metallurgical Engineering Department and Barcelona Research Center in Multiscale Science and Engineering, EEBE, Technical University of Catalonia (UPC), Av. Eduard Maristany 16, 08019 Barcelona (Spain).

[4] Serra Húnter Fellowship, Generalitat de Catalunya (Spain).

ABSTRACT

Since nitrate (NO_3^-) has been related to human health and environmental problems, safe and sustainable strategies to remediate polluted water bodies must be investigated. This work aims to assess the feasibility of using ferrous iron (Fe(II))-containing minerals to stimulate microbial denitrification while avoiding pollution swapping (e.g. accumulation of the by-products nitrite (NO_2^-) or nitrous oxide (N_2O)). To accomplish the objective, samples obtained from several batch experiments were

characterized chemically and isotopically. Magnetite, siderite and olivine were tested micro-sized and magnetite was also tested nano-sized. In microbial experiments, NO_3^- polluted groundwater was employed as inoculum. In these experiments, NO_3^- reduction to nitrogen gas (N_2) was only completed in microcosms containing magnetite nanoparticles, suggesting an increased Fe(II) availability from nano-sized compared to micro-sized magnetite. In abiotic experiments, no reactivity was observed between NO_3^- or NO_2^- and micro-sized magnetite, siderite or olivine, while NO_2^- was rapidly reduced when dissolved Fe^{2+} was added. These results point to the need of a certain amount of dissolved Fe^{2+} to stimulate the abiotic NO_2^- reduction by Fe(II) oxidation. For the microbial NO_3^- reduction by magnetite nanoparticles, the calculated $\varepsilon^{15}N_{NO3}$ was -33.1 ‰ (R^2 = 0.86), $\varepsilon^{18}O_{NO3}$ was -10.7 ‰ (R^2 = 0.74) and $\varepsilon^{15}N_{NO3}/\varepsilon^{18}O_{NO3}$ was 3.1. For the abiotic NO_2^- reduction by Fe^{2+}, the $\varepsilon^{15}N_{NO2}$ ranged from -14.1 to -17.8 ‰ (R^2 > 0.89). Considering the wide range of $\varepsilon^{15}N_{NO2}$ reported in the literature, it is not likely that NO_2^- isotopic characterization can be useful at field-scale to distinguish abiotic from microbial NO_2^- reduction. Nevertheless, the measured $\delta^{15}N$ for N_2O in microbial and abiotic tests, allowed to determine if it was an intermediate or a final product of the reactions by comparing these results with the modelled isotopic composition calculated using the $\varepsilon^{15}N$ values determined for the substrates. Hence, isotopic data confirmed that the product of the microbial NO_3^- reduction was innocuous N_2 while the product of the abiotic NO_2^- reduction was N_2O. The latter reaction would be advantageous to avoid NO_2^- accumulation during denitrification only if the generated N_2O is further reduced by microorganisms.

Keywords: abiotic nitrite reduction, denitrification, isotopic fractionation, magnetite nanoparticles, nitrous oxide

1. INTRODUCTION

Nitrate (NO_3^-) has been related to human health disorders such as cancer and blue baby syndrome and to environmental problems such as eutrophication of water bodies (Rivett et al., 2008; Vitousek et al., 1997; Ward et al., 2005). Due to decades of excessive crop fertilization and septic system leakage, NO_3^- is widely found in groundwater. Consequently, since 1991, European directives (2006/118/EC, 2006; 91/676/EEC, 1991; 98/83/EC, 1998) have arisen to face the NO_3^- pollution persistence. One of the measures that can be implemented to attenuate the NO_3^- concentration in water bodies is the addition of external electron donors to promote the denitrification, since these compounds are usually deficient at field-scale (Rivett et al., 2008). The NO_3^- is reduced to innocuous nitrogen gas (N_2) simultaneously to the oxidation of an electron donor by denitrifying microorganisms (Borden et al., 2012; Böttcher et al., 1990; Otero et al., 2009; Smith et al., 2001). However, intermediate N compounds can be generated and accumulated since denitrification occurs through a series of enzymatic reactions involving the conversion of NO_3^- to nitrite (NO_2^-), nitric oxide (NO), nitrous oxide (N_2O) and finally N_2 (Betlach and Tiedje, 1981; Knowles, 1982; Vidal-Gavilan et al., 2013; Weymann et al., 2010). Not only NO_3^- but also these intermediate N compounds have been recognized to produce detrimental effects for the environment and human health (Badr and Probert, 1993; Vitousek et al., 1997; Ward et al., 2005). Therefore, pollution swapping should be avoided when stimulating denitrification at field-scale.

In the search of economical and sustainable electron donors at laboratory-scale, diverse industrial and agricultural waste products rich in organic carbon (C) have proved to stimulate heterotrophic denitrification (Carrey et al., 2018; Gibert et al., 2008; Margalef-Marti et al., 2019b; Si et al., 2018; Trois et al., 2010), while ferrous iron (Fe(II))-containing minerals such as pyrite, pyrrothite or biotite showed to stimulate lithoautotrophic denitrification (Aquilina et al., 2018; Bosch et al., 2012; Torrentó et al.,

2011; Yan et al., 2019; Yang et al., 2017). In the case of pyrite, it has been recently suggested that NO_3^- reduction might be stimulated by S instead of Fe oxidation (Yan et al., 2019). Also, a potential NO_3^- reactivity with the Fe(II,III) minerals green rust and magnetite has been observed (Byrne et al., 2015; Dhakal et al., 2013; Pantke et al., 2012). On the other hand, since mineral nanoparticles (NP) (e.g. Fe(III)(oxyhydr)oxides) are usually more reactive than macroparticles, their potential use to remediate polluted water bodies has gained attraction during the last years (Braunschweig et al., 2013). Materials such as Fe(0)-NP, magnetite-NP, Fe(III)oxide-NP or magnetite/maghemite-NP have been found to remove different organic and inorganic contaminants (Chowdhury and Yanful, 2010; Crane et al., 2011; Zelmanov and Semiat, 2008). Regarding NO_3^-, pyrite-NP, zeolite supported Fe/Ni-NP and Fe(0)/magnetite-NP could attenuate the pollution (Bosch et al., 2012; Cho et al., 2015b, 2015a; He et al., 2018).

In the aforementioned microbial denitrification studies, a transient NO_2^- accumulation was generally observed (Ge et al., 2012; Torrentó et al., 2011; Yang et al., 2017), and although the gas emissions were not measured, N_2O accumulation cannot be discarded since this greenhouse gas (GHG) is usually detected during NO_3^- reduction both at laboratory and field-scale (Jurado et al., 2017; Margalef-Marti et al., 2019a; Morley et al., 2008; Weymann et al., 2010). During the last years, numerous studies have pointed that abiotic reactions involving the N and Fe biogeochemical cycles occur simultaneously to microbial denitrification (Carlson et al., 2013; Klueglein and Kappler, 2013; Matocha and Coyne, 2007; Melton et al., 2014). The abiotic reduction of NO_2^- by Fe(II) oxidation have been well documented (Buchwald et al., 2016; Dhakal et al., 2013; Grabb et al., 2017; Rakshit et al., 2016), and might be advantageous to avoid a water quality decrease due to NO_2^- accumulation. However, N_2O has been proposed as the final product of this reaction (Buchwald et al., 2016; Chen et al., 2018; Coby and Picardal, 2005; Wang et al., 2016). Hence, supplying NO_3^- polluted water bodies with

Fe(II)-containing minerals to stimulate lithoautotrophic denitrification might promote N_2O generation from both the microbial and abiotic NO_2^- reduction. In laboratory experiments, Cooper et al. (2003) already found a larger N_2O production during denitrification in the presence of Fe(II) compared to absence. Nevertheless, the accumulated N_2O by both microbial and abiotic pathways could be further reduced by microorganisms in the presence of electron donors. The relative contribution of these two pathways of N_2O production should be carefully assessed since the GHG is currently a focus of attention in climate change research (Reay et al., 2012).

The analysis of stable isotopes coupled to hydrochemical investigations is a widely accepted approach to understand biogeochemical processes in water bodies. The enzymatic NO_3^- reduction provokes an enrichment in the heavy isotopes ^{15}N and ^{18}O of the unreacted substrate, unlike processes such as dilution that leads to a concentration decrease without influencing the isotopic signature (Böttcher et al., 1990; Fukada et al., 2003; Mariotti et al., 1981; Aravena and Robertson, 1998). The same pattern is expected throughout the enzymatic reduction of all N intermediate products (e.g. NO_2^- or N_2O), which will be initially depleted in ^{15}N and ^{18}O with respect to the substrate until the ultimate product will reach the NO_3^- initial isotopic composition. Although the NO_3^- isotopic evolution through heterotrophic denitrification has been widely studied (Carrey et al., 2014; Granger et al., 2008; Grau-Martínez et al., 2017; Wunderlich et al., 2012), the characterization during lithoautotrophic denitrification is scarce (Torrentó et al., 2011, 2010). Furthermore, information on the dual isotope systematics of NO_2^- and N_2O throughout its abiotic reduction by Fe(II) is still limited (Buchwald et al., 2016; Chen et al., 2018; Grabb et al., 2017; Jones et al., 2015). Therefore, it is not clear to which extent the isotopic characterization of NO_3^-, NO_2^- and N_2O might help in distinguishing microbial and abiotic reactions involving the N and Fe biogeochemical cycles.

In this context, the aim of this work was to assess at laboratory-scale the suitability of using different Fe(II)-containing minerals to stimulate NO_3^- reduction in groundwater (e.g. in permeable reactive barriers or by injection), while avoiding pollution swapping. The selected minerals were magnetite (Mag), siderite (Sd) and olivine (Ol), which were tested micro-sized. Mag was also tested nano-sized, to check changes in reactivity. Special attention was directed on the generation, accumulation and further reduction of the by-products NO_2^- and N_2O throughout the microbial NO_3^- reduction. For this reason, the potential abiotic reactivity between NO_3^- or NO_2^- and Fe(II)-containing minerals or dissolved Fe^{2+} was also evaluated. To accomplish the objective, the samples obtained from several batch experiments were characterized chemically and isotopically.

2. METHODS

2.1. Batch experiments

Micro-sized Mag, Ol and Sd and Mag-NP were tested to assess its potential use to stimulate microbial NO_3^- reduction in laboratory batch experiments simulating aquifer conditions. Groundwater was obtained from well SMC-002 located in Roda de Ter (Barcelona, Spain). In this area, lithoautotrophic denitrification occurrence has been reported previously (Hernández-del Amo et al., 2018; Otero et al., 2009; Vitòria et al., 2008). In groundwater collected from the SMC-002 well, genes encoding the NO_2^- and N_2O reductases (nirS, nirK, and nosZ1) have also been detected and certain genus of denitrifying and Fe(II) oxidizing bacteria have been identified (Hernández-del Amo et al., 2018). Furthermore, aquifer geological material (mudstone) obtained from a similar nearby aquifer system was milled and then added in these microcosms to increase microbial diversity (hereafter named sediment). Hence, the series of experiments BioSedGW contained sediment, groundwater (1 mM NO_3^-) and one of the selected minerals. Instead, the series BioSedDIW contained sediment, deionized water with

$NaNO_3$ (1 mM) and one of the selected minerals, which was employed as a control, to check a possible contribution of the sediment on the stimulated denitrification in the BioSedGW experiments. For the BioSedDIW experiments, it was assumed that denitrifying microorganisms were negligible in the deionized water and that the different chemical composition between deionized water and groundwater would not impart a significant effect on the sediment compounds dissolution. Both the BioSedGW and BioSedDIW series included a control without mineral. In addition, three bottles containing sediment and MilliQ water were incubated to determine a possible leakage of organic C from the sediment (blank experiments).

Micro-sized Mag, Ol and Sd were also tested to assess its potential abiotic reactivity with NO_3^- and NO_2^-. Three series of parallel anoxic incubations were performed. The series AbFeNO_3 contained NO_3^- rich synthetic water (1 mM), one of the three selected minerals and dissolved Fe^{2+}. The series AbFeNO_2 contained NO_2^- rich synthetic water (1 mM), one of the three selected minerals and dissolved Fe^{2+}. In both series dissolved Fe^{2+} was added to maximize Fe(II) availability from a filtered $FeCl_2 \cdot 4H_2O$ aqueous solution (5 mM). Finally, the series AbNO2 contained NO_2^- rich synthetic water (1 mM) and one of the three selected minerals.

The detailed composition of each series of experiments is shown in **Table 1**. The main experiments (BioSedGw) involved 8 bottles for each mineral tested, two additional bottles were included in the case of Mag-NP. In contrast, the control experiments involved just 3 bottles, except for the Ab$FeNO_2$ series that also involved 8 bottles to allow characterizing the abiotic NO_2^- reduction. The five series of batch experiments were set up inside a glove box, using 20 mL serum bottles, crimp sealed with butyl rubber stoppers under an Ar atmosphere. Incubations were performed at 23 ºC and constant shaking in the darkness to avoid photodegradation processes. The bottles were sacrificed by turns at time intervals depending on the NO_3^- and NO_2^- reduction dynamics.

The characterization of the different types of water employed in the study is shown in the Supporting Information **Table S1**. The micro-sized minerals (Mag, Sd and Ol) preparation and Mag size reduction is explained in the Supporting Information **Section S1**. The mineral characterization is detailed in the Supporting Information **Section S2**.

2.2. Analytical techniques

All samples from the sacrificed bottles were filtered through 0.2 µm Millipore® filter immediately when obtained and stored at 4 ºC until analysis except aliquots for ammonium (NH_4^+) concentration and isotopic characterization of N and O from dissolved NO_3^- and NO_2^- that were preserved frozen at -20 ºC. Samples from experiments $AbFeNO_3$ and $AbFeNO_2$ were analyzed immediately when obtained.

Concerning the chemical analyses, concentrations of NO_3^- and NO_2^- were analyzed by high performance liquid chromatography (HPLC, WATERS 515 pump and WATERS IC-PAK ANIONS column with WATERS 432 and UV/V KONTRON detectors). Exceptionally, in the $AbFeNO_2$ experiments, NO_2^- concentration was calculated from the isotope ratio mass spectrometer (IRMS) peak areas results. Due to the high abiotic NO_2^- reduction rates, NO_2^- reduction to N_2O by a sodium azide solution with acetic acid (McIlvin and Altabet, 2005; Ryabenko et al., 2009) immediately after samples collection, followed by IRMS analysis, provided a reliable method to ensure that NO_2^- was not further reduced or oxidized to NO_3^- during preservation or lag time needed for other methods (such as HPLC). The NH_4^+ concentration was determined by spectrophotometry (CARY 1E UV-visible) using the indophenol blue method ($AbFeNO_2$ experiments) (Bolleter et al., 1961) or by ionic chromatography (BioSedGW and BIoSedDIW experiments). The N_2O accumulated at the head-space of the vials was measured by gas chromatography (GC) with an electron capture detector (ECD) (Thermo Scientific, Trace 1300). The NPDOC was analyzed by organic matter combustion (TOC 500 SHIMADZU). The dissolved Fe and trace elements were

determined by inductively coupled plasma optical emission spectrometry (ICP-OES, Perkin Elmer Optima 8300 and Perkin Elmer Optima 3200 RL).

The $\delta^{15}N\text{-}NO_3^-$, $\delta^{18}O\text{-}NO_3^-$ and $\delta^{15}N\text{-}NO_2^-$ compositions were determined following the cadmium and azide reduction methods (McIlvin and Altabet, 2005; Ryabenko et al., 2009). The first step of this method consists on NO_3^- reduction to NO_2^- in columns filled with cadmium pearls. The second step consists on NO_2^- reduction to N_2O in crimp sealed vials, in which a sodium azide solution with acetic acid is added. The isotopic composition of the generated N_2O through this method or collected from the headspace of the microcosms was analyzed using a Pre-Con (Thermo Scientific) coupled to an IRMS (Finnigan MAT 253, Thermo Scientific). Notation is expressed in terms of δ (‰) relative to the international standards: Atmospheric N_2 (AIR) for $\delta^{15}N$ and Vienna Standard Mean Oceanic Water (V-SMOW) for $\delta^{18}O$. Hence, $\delta = (R_{sample}\text{-}R_{standard})/R_{standard}$, where R is the ratio between the heavy and the light isotopes. According to Coplen (2011), several international and laboratory (UB) standards were interspersed among samples for normalization of the results: USGS-51, USGS-32, USGS-34, USGS-35, UB-$NaNO_3$ ($\delta^{15}N$ = +16.9 ‰, $\delta^{18}O$ = +28.5 ‰) and UB-KNO_2 ($\delta^{15}N$ = +28.5 ‰). The reproducibility (1σ) of the samples, calculated from the standards systematically interspersed in the analytical batches, was ±1.0 ‰ for $\delta^{15}N\text{-}NO_3^-$, ±1.5 ‰ for $\delta^{18}O\text{-}NO_3^-$, ±0.5 for $\delta^{18}O\text{-}NO_2^-$ and ±0.1 for $\delta^{15}N\text{-}NO_2^-$.

Chemical and isotopic analyses were prepared at the laboratory of the MAiMA-UB research group and analyzed at the Centres Científics i Tecnològics of the Universitat de Barcelona (CCiT-UB).

2.3. Isotopic fractionation calculation

Under closed system conditions, the isotopic fractionation ($\varepsilon^{18}O$ and $\varepsilon^{15}N$) can be calculated by means of a Rayleigh distillation equation (**Equation 1**) (Böttcher et al., 1990; Mariotti et al., 1988). Thus, ε can be obtained from the slope of the linear

correlation between the natural logarithm of the substrate remaining fraction ($Ln(C_{residual}/C_{initial})$, where C refers to analyte concentration) and the determined isotope ratios ($Ln(R_{residual}/R_{initial})$, where $R = (\delta+1)$).

$$\ln\left(\frac{R_{residual}}{R_{initial}}\right) = \varepsilon \times \ln\left(\frac{C_{residual}}{C_{initial}}\right) \quad \textbf{Equation 1}$$

3. RESULTS AND DISCUSSION

All data obtained from the laboratory experiments is reported in the Supporting Information **Table S2**.

3.1. Microbial NO_3^- reduction by Fe(II)-containing minerals

During the first week of incubation, in the microbial experiments containing groundwater or deionized water with NO_3^-, plus sediment, plus minerals (BioSedGW-Min and BioSedDIW-Min), the NO_3^- concentration decreased by 30-60 % of the initial values (**Figures 1A and 1B**). Attenuation of NO_3^- was also observed in the BioSedGW-C microcosms that lacked mineral (up to 40 % NO_3^- reduction). Therefore, the beginning of denitrification was likely caused by heterotrophic bacteria that used the organic C from both sediment and groundwater as electron donor. In blank experiments containing only MilliQ water and sediment, 0.4 ± 0.03 mM NPDOC leaked from this sediment, which has to be added to the 0.2 mM NPDOC already present in groundwater in the BioSedGW experiments. At the beginning of microbial NO_3^- reduction, NO_2^- usually accumulates until bacterial communities adapt to the new redox conditions caused by the electron donor addition. This can be explained by an earlier induction of NO_3^- reductases with respect to NO_2^- reductases that could provoke lower initial NO_2^- reduction rates. Hence, the main parameters affecting NO_2^- accumulation are the initial inoculum, the type of electron donor involved and its molar ratio with respect to NO_3^- (Akunna et al., 1993; Betlach and Tiedje, 1981; Ge et al., 2012; Zumft,

1997). The lower NO_2^- accumulation found in BioSedGW-Min microcosms (up to 0.2 mM) compared to BioSedDIW-Min microcosms (up to 0.6 mM) is therefore consistent with a higher NPDOC content and inoculum in BioSedGW (groundwater + sediment) compared to BioSedDIW microcosms (just sediment) (**Figures 1C and 1D**).

After the first week, NO_3^- or NO_2^- concentrations did not change significantly in the BioSedDIW experiments (**Figures 1B and 1D**). In the BioSedGW microcosms with micro-sized (Mag, Ol, Sd) or lacking minerals (C), significant differences in NO_3^- concentration were not observed (**Figure 1A**), but from day 118 on, NO_2^- was no longer detected (**Figure 1C**). These results suggested that organic C from sediment and groundwater and available Fe(II) from micro-sized minerals were insufficient to complete NO_3^- reduction to N_2. Also, that the higher microbial inoculum and dissolved organic C content in BioSedGW experiments allowed an extended progression of the reaction compared to BioSedDIW experiments. In contrast, in the BioSedGW-Mag-NP microcosms, about 96 % NO_3^- reduction was achieved in 91 days (**Figure 1A**), showing transient NO_2^- accumulation (up to 0.2 mM) until day 91 (**Figure 1C**). In the BioSedGW microcosms, NH_4^+ concentration was below 0.04 mM, discarding a major contribution of dissimilatory NO_3^- reduction to ammonium (DNRA) and suggesting that the end products of NO_3^- reduction were gaseous N compounds. The measured N_2O at the head-space of the BioSedGW vials was below 0.1 % of the initial N in the control, below 0.4 % in the micro-sized minerals microcosms, and below 0.8 % in the Mag-NP microcosms. The highest concentration being detected in the BioSedGW-Mag-NP microcosms is consistent with the highest reduction being observed in these batches. The low percentage of N in form of N_2O found in the BioSedGW experiments suggested that the final gaseous product of the microbial NO_3^- reduction was N_2, either during the initial heterotrophic activity and as a result of the denitrification stimulated by Mag-NP. Therefore, if during the denitrification stimulated by Mag-NP, an abiotic reactivity between NO_2^- and the available Fe(II) occurred, the produced N_2O seemed to

be further reduced to N_2 by microorganisms. Similarly, in a NO_3^- polluted aquifer in the presence of Fe(II) and low organic C, the results obtained by Smith et al. (2017) suggested that NO_3^- was reduced both heterotrophically and lithoautotrophically while NO_2^- was also reduced abiotically and the generated N_2O was further reduced to N_2 by microorganisms down-gradient.

Our results suggest that Mag-NP allowed a higher structural Fe(II) availability with respect to micro-sized Mag due to an increased surface area coupled to a decreased grain size (Supporting Information **Section S2**). Similar to our results, Aquilina et al. (2018) and Yang et al. (2017) related an increased denitrification rate to a decreased grain size of minerals (granite-biotite and pyrrothite, respectively). Smaller particles usually enhance mineral solubility, which might accelerate microbial reduction rates. Braunschweig et al. (2013) even suggested that in case of nanoparticles precipitation, the solubility might be independent of the aggregate size. However, dissolved Fe^{2+} concentration was below detection limit in almost all samples of our microbial experiments. Bacteria likely oxidized either structural Fe(II) or adsorbed Fe(II) on mineral surface. Alternatively, if Fe^{2+} was released through dissolution, bacteria immediately oxidized it to Fe(III), which precipitated and became unavailable for detection. The ICP results (Supporting Information **Table S2.2**), neither proved a possible mineral dissolution. The Mag Fe(II)/Fe(III) stoichiometry can also influence its reactivity (Gorski et al., 2010). Nevertheless, during the protocol followed to obtain nano-sized from micro-sized Mag we did not expect a variation in the Fe(II)/Fe(III) ratio (Supporting Information **Section S2**). Hence, we discarded this factor as a main contributor for the observed changes in reactivity between the two different Mag grain sizes tested in our experiments. On the other hand, considering that not all structural Fe(II) was available for reduction, the Fe(II)/N molar ratio in the micro-sized minerals experiments was likely too low to complete NO_3^- reduction, especially in the case of Sd and Ol (initial Fe(II)/N of 13 and 7, respectively compared to 24 calculated for Mag and

Mag-NP). In a study with *Microbacterium* sp. W5, 90 % NO_3^- removal was achieved when using a Fe(II)/N ratio of nearly 30, which is far above from the stoichiometric ratio of 5 (Zhou et al., 2016).

In a previous study, in groundwater collected from the SMC-002 well, Hernández-del Amo et al. (2018) identified at genus level *Sideroxydans*, *Acidiferrobacter* and *Thiobacillus* species, which are capable of Fe(II) oxidation and NO_3^- reduction, and *Nitrospira*, *Geobacillus* and *Solitalea* species, which are also capable to reduce NO_3^-. Bacterial species involved in these genera could have stimulated the NO_3^- reduction observed in the BioSedGW experiments since groundwater collected from the same well was employed. The microbial NO_3^- dependent Fe(II) oxidation (NDFO) mechanisms, are not still completely understood (Bryce et al., 2018; Price et al., 2018; Straub et al., 1996). Among the microorganisms that have been related to NDFO, lithoautotrophs have been identified but most of them are mixotrophic, requiring an organic C co-substrate for growth, or even the NDFO can result from a synergistic activity between different NO_3^- reducing and Fe(II) oxidizing microorganisms (Bryce et al., 2018; Melton et al., 2014; Price et al., 2018; Weber et al., 2006). Some authors propose that NDFO mixotrophic communities might need a lower organic C supply to reduce NO_3^- compared to heterotrophic communities (Devlin et al., 2000; He et al., 2016). Hence, we could not discard the simultaneous use of organic C from sediment and groundwater and Fe(II) from minerals in our microbial experiments with Mag-NP, Mag, Ol or Sd.

3.2. NO_3^- and NO_2^- abiotic reactivity with Fe(II)

The abiotic experiments containing synthetic water with NO_3^- and dissolved Fe^{2+} plus micro-sized Mag, Ol or Sd (AbFeNO_3) showed a lack of significant reactivity (**Figure 2A**). This lack of reactivity was also observed in qualitative previous tests performed with NO_3^- and the micro-sized minerals without addition of dissolved Fe^{2+} (Supporting

Information **Table S2.8**). These results reinforced that the NO_3^- reduction observed in our microbial experiments (BioSedGW and BioSedDIW) was caused by biological activity.

The abiotic experiments containing synthetic water with NO_2^- plus the micro-sized Mag, Ol and Sd ($AbNO_2$) also showed a lack of significant reactivity (**Figure 2B**). However, a rapid NO_2^- reduction was observed in the abiotic experiments containing synthetic water with NO_2^- and dissolved Fe^{2+} involving the lack (C) or addition of the micro-sized Mag, Ol and Sd ($AbFeNO_2$) (**Figure 3A**). The beginning of the reaction seemed to be immediate and NO_2^- removal was completed in both the $AbFeNO_2$-Min and $AbFeNO_2$-C experiments, which is consistent with previous studies showing a significant NO_2^- reduction (approximately 60 % in 4 days) even at an equimolar dissolved Fe^{2+}/NO_2^- molar ratio (Jones et al., 2015). A faster reduction (~ 50 hours) was observed in the experiments containing Sd compared to those without mineral or with Mag or Ol (~ 175 hours), possibly due to an increased Fe(II) availability in Sd. Since the measured NH_4^+ was below 0.05 mM, it was considered that NO_2^- was reduced to gaseous products. As previously observed by other authors, N_2O accumulated at the headspace of the batches as a result of the NO_2^- abiotic reduction by Fe(II) oxidation (Buchwald et al., 2016; Chen et al., 2018; Coby and Picardal, 2005; Wang et al., 2016). Our results point that N_2O was the end product because a mass balance between the remaining NO_2^- in the solution and the accumulated N_2O in the headspace for each vial was close to the NO_2^- initial value (**Figure 3B**). Kampschreur et al. (2011) observed a complete recovery of NO_2^- as NO and N_2O. Hence, the missing mass balance complement to N_2O is likely to be found as NO. According to these results, if Fe(II)-containing minerals are applied in polluted water bodies to promote denitrification, NO_2^- accumulation could be avoided after its abiotic reduction in the presence of dissolved Fe^{2+}. However, this NO_2^- abiotic reduction would be beneficial only if the generated N_2O is further reduced by microorganisms.

In these $AbFeNO_2$ experiments, a dissolved Fe^{2+} decrease was observed in accordance to NO_2^- reduction from the initial 5 mM to approximately 2 mM, showing no significant differences between the experiment without mineral or the ones with micro-sized Mag, Ol or Sd (**Figure 3C**). Total dissolved Fe measured by ICP-OES was considered to be solely dissolved Fe^{2+} since Fe(III) was quickly precipitated and because the ICP-OES method have previously shown equal results compared with ferrozine analysis (Smith et al., 2017). In studies focusing on the abiotic NO_2^- reduction coupled to Fe(II) oxidation, homogeneous reactions produced by oxidation of dissolved Fe^{2+} are distinguished from heterogeneous reactions in which Fe(II) is associated to mineral or bacterial surfaces or found as structural Fe(II) within minerals. Some studies suggest that a faster NO_2^- reduction is produced through the heterogeneous reaction (Buchwald et al., 2016; Dhakal et al., 2013) although low or null dissolved Fe^{2+} concentrations can inhibit NO_2^- reduction even in the presence of mineral-associated Fe(II) (Tai and Dempsey, 2009). This is consistent with the lack of reactivity found for the $AbNO_2$ compared to the $AbFeNO_2$ experiments.

3.3. Isotopic characterization

3.3.1. Isotopic fractionation of NO_3^- during microbial reduction

The initial isotopic values measured in groundwater of +11.3 ‰ for $\delta^{15}N\text{-}NO_3^-$ and +10.1 ‰ for $\delta^{18}O\text{-}NO_3^-$ increased to +158.1 ‰ and +47.5 ‰, respectively, throughout the microbial NO_3^- reduction stimulated by the Mag-NP (BioSedGW-Mag-NP). The calculated $\varepsilon^{15}N_{NO3}$ was -33.1 ‰ (R^2 = 0.86) and $\varepsilon^{18}O_{NO3}$ was -10.7 ‰ (R^2 = 0.74) (**Figure 4A**), giving a $\varepsilon^{15}N_{NO3}/\varepsilon^{18}O_{NO3}$ of 3.1. While this $\varepsilon^{18}O_{NO3}$ is within the range of values reported for microbial denitrification experiments at laboratory-scale, the $\varepsilon^{15}N_{NO3}$ and the $\varepsilon^{15}N_{NO3}/\varepsilon^{18}O_{NO3}$ are found in the highest extreme (absolute values) (see **Table 2**). Similar $\varepsilon^{15}N_{NO3}$ were reported by Torrentó et al. (2011) in batch experiments using aquifer material and pyrite (-27.6 ‰) and by Tsushima et al. (2006) in column

experiments using riparian aquifer sediments (-34.1 ‰). However, Torrentó et al. (2011) obtained a $\varepsilon^{15}N_{NO3}/\varepsilon^{18}O_{NO3}$ close to 1 and Tsushima et al. (2006) did not report values for $\varepsilon^{18}O_{NO3}$. Likely due to $\delta^{18}O\text{-}NO_2^-$ equilibration with $\delta^{18}O\text{-}H_2O$ and subsequent NO_2^- reoxidation to NO_3^-, Knöller et al. (2011) found a $\varepsilon^{15}N_{NO3}/\varepsilon^{18}O_{NO3}$ of 3 ($\varepsilon^{15}N_{NO3}$ = -16.2 ‰ and $\varepsilon^{18}O_{NO3}$ = -5.5 ‰), using succinate as electron donor and *Pseudomonas pseudoalcaligenes*. These results might be coherent with our results after such a long incubation and important NO_2^- accumulation. After $\delta^{18}O\text{-}NO_2^-$ exchange with $\delta^{18}O\text{-}H_2O$, which ranges between -4 and -7 ‰ in the area where the SMC-002 well is placed, if NO_2^- reoxidates to NO_3^-, a decreased $\delta^{18}O\text{-}NO_3^-$ enrichment might be expected compared to the $\delta^{15}N\text{-}NO_3^-$ enrichment. Therefore, the resulting $\varepsilon^{15}N_{NO3}/\varepsilon^{18}O_{NO3}$ might be higher than those close to 1.0 usually resulting from NO_3^- reduction to NO_2^- and subsequent reduction to gaseous products. If a bioremediation strategy by using Mag-NP to promote denitrification is implemented, the calculated ε values in the present study could be applied to evaluate the efficiency of the treatment (Margalef-Marti et al., 2019c; Meckenstock et al., 2004; Vidal-Gavilan et al., 2013). However, due to the $\delta^{18}O\text{-}NO_2^-$ exchange with $\delta^{18}O\text{-}H_2O$, calculations derived from $\varepsilon^{18}O_{NO3}$ might be used with caution.

In the case of the microbial experiments containing micro-sized minerals (BioSedGW-Mag/Ol/Sd), an isotopic fractionation during the initial uncomplete denitrification was also observed. These isotopic results are presented as a whole since a similar trend was found for the different tested conditions, which is explained by the use of NPDOC released from sediment and groundwater as electron donor in all cases. Calculated $\varepsilon^{15}N_{NO3}$ was -12.0 ‰ (R^2 = 0.56) and $\varepsilon^{18}O_{NO3}$ was -10.9 ‰ (R^2 = 0.63) (**Figure 4B and 4D**), giving a $\varepsilon^{15}N_{NO3}/\varepsilon^{18}O_{NO3}$ of 1.1. These values are within the range reported for microbial denitrification in laboratory-scale experiments (see **Table 2**) and point to a lack of NO_2^- reoxidation in contrast to the Mag-NP experiments. The main reason for the NO_2^- reoxidation occurrence only in the Mag-NP experiments could be the longer

incubation time and therefore, longer persistence of NO_2^- accumulation. This long persistence of NO_2^- could have let enough time for activation of the enzymatic NO_2^- oxidation. In the groundwater employed for the experiments, bacterial species from the genus *Nitrospira* were identified (Hernández-del Amo et al., 2018). Microorganisms from this genus have been previously related to both nitrification and denitrification activity and could have allowed both NO_2^- reduction and oxidation (Koch et al., 2015).

3.3.2. Isotopic fractionation of N-NO_2^- during the abiotic reduction

In the abiotic NO_2^- reduction experiments with dissolved Fe^{2+} with or without micro-sized minerals ($AbFeNO_2$), the initial δ^{15}N-NO_2^- of -28.5 ‰ increased to -16.8 ‰, -14.9 ‰, -14.5 ‰ and +7.1 ‰ in the C, Mag, Sd and Ol batches, respectively. No significant differences were observed in the calculated $\varepsilon^{15}N_{NO2}$ for these experiments (**Figure 4C**), suggesting that the observed NO_2^- abiotic reduction was mainly caused by dissolved Fe^{2+} oxidation. The $\varepsilon^{15}N_{NO2}$ values were -14.1 ‰ (R^2 = 0.92) for the $AbFeNO_2$-C, -14.1 ‰ (R^2 = 0.99) for Sd, -14.6 ‰ (R^2 = 0.89) for Mag and -17.8 ‰ (R^2 = 0.95) for Ol. In these experiments, the $\varepsilon^{18}O_{NO2}$ was not calculated because no clear δ^{18}O-NO_2^- enrichment coupled to NO_2^- reduction was observed, pointing to δ^{18}O-NO_2^- equilibration with δ^{18}O-H_2O. In similar studies, a possible contribution from δ^{18}O-NO_2^- equilibration with δ^{18}O-H_2O could not be discarded (Buchwald et al., 2016; Grabb et al., 2017), and Jones et al. (2015) also found a weaker δ^{18}O-NO_2^- enrichment compared to the δ^{15}N-NO_2^- enrichment ($\varepsilon^{18}O_{NO2}$ = 10 ‰ vs $\varepsilon^{15}N_{NO2}$ = 13 ‰, respectively). These authors proposed an exchange between δ^{18}O-NO_2^- and δ^{18}O-H_2O since de δ^{18}O-NO_2^- continued to variate after the abiotic NO_2^- reduction was stopped.

Testing the NO_2^- abiotic reduction with different incubation conditions, other authors have reported $\varepsilon^{15}N_{NO2}$ values ranging from -2.3 ‰ to -44.8 ‰, $\varepsilon^{18}O_{NO2}$ from -4.1 ‰ to -33.0 ‰, and $\varepsilon^{15}N_{NO2}/\varepsilon^{18}O_{NO2}$ between 0.5 and 1.6 (see **Table 2**). Our $\varepsilon^{15}N_{NO2}$ results fall within this wide range. Although different isotopic trends were found between NO_2^-

reduction caused by structural Fe(II) or Fe(II) adsorbed onto mineral surfaces or dissolved Fe^{2+} in the laboratory studies performed by Buchwald et al. (2016) and Grabb et al. (2017), we did not observe such difference. Considering the wide range of reported ε values, it is not likely that the NO_2^- isotopic characterization could be useful at field-scale to distinguish the homogeneous and heterogeneous reactions. Furthermore, $\varepsilon^{15}N_{NO2}$ and $\varepsilon^{18}O_{NO2}$ within this range have also been reported for the microbial NO_2^- reduction, which resulted in $\varepsilon^{15}N_{NO2}/\varepsilon^{18}O_{NO2}$ between 0.7 and 22.0 (see **Table 2**). Therefore, the NO_2^- isotopic characterization may neither be useful at field-scale to distinguish the abiotic from the microbial NO_2^- reduction.

3.3.3. Isotopic evolution of N_2O in microbial and abiotic experiments

The isotopic composition of the accumulated N_2O in the microbial NO_3^- reduction experiments showed variations. Neither N_2O nor NO_3^- concentrations presented a clear relationship with the determined $\delta^{15}N\text{-}N_2O$ or $\delta^{18}O\text{-}N_2O$ due to the simultaneous production and reduction of this intermediate product of denitrification. However, a correlation was observed between $\delta^{18}O\text{-}N_2O$ and $\delta^{15}N\text{-}N_2O$, giving slopes ranging from -2.4 to +2.3 for the BioSedGW-Min experiments (**Figures 5A and 5B**). Given the lack of studies reporting an exhaustive isotopic characterization of nitrous oxide during the autotrophic denitrification, we don't have consistent hypothesis to explain why the micro-sized Mag gave an inverse slope compared to Ol and Sd. We think that the isotopic characterization of N_2O during its simultaneous production and reduction during denitrification require further investigation.

The $\delta^{15}N\text{-}N_2O$ ranged from -11.1 ‰ to +63.4 ‰ and the $\delta^{18}O\text{-}N_2O$ from -3.5 ‰ to +62.6 ‰ in the BioSedGw-Mag-NP experiments, while in the BioSedGW experiments containing micro-sized minerals, the $\delta^{15}N\text{-}N_2O$ ranged from -31.3 ‰ to +5.1 ‰ and the $\delta^{18}O\text{-}N_2O$ from -12.0 ‰ to +52.4 ‰. The increased variation of the $\delta^{15}N\text{-}N_2O$ in the BioSedGw-Mag-NP compared to the BioSedGW-Mag/Ol/Sd and the similar $\delta^{18}O\text{-}N_2O$

enrichment between the BioSedGw-Mag-NP and the BioSedGW-Mag/Ol/Sd, is consistent with the obtained ε values for the substrates. Moving to the abiotic experiments with dissolved Fe^{2+} with or without micro-sized minerals ($AbFeNO_2$), a lower variation in the $\delta^{15}N\text{-}N_2O$ was observed compared to the microbial experiments (**Figure 5C**). In these abiotic experiments, it is likely that during the beginning of N_2O production the $\delta^{15}N\text{-}N_2O$ decreases and afterwards increases (e.g. initial N_2O produced in the $AbFeNO_2$-Mag experiments presents a $\delta^{15}N\text{-}N_2O$ of -48.4 ‰ that decreases to -53.8 ‰ and then increases to -43.4 ‰). Because the $\delta^{18}O\text{-}NO_2^-$ in these experiments presented equilibration with $\delta^{18}O\text{-}H_2O$, the $\delta^{18}O\text{-}N_2O$ results did not provide valuable information.

Since a much higher $\delta^{15}N\text{-}N_2O$ variation was observed for the microbial experiments compared to the abiotic experiments, observing important $\delta^{15}N\text{-}N_2O$ variations in denitrification studies could be indicative of microbial activity. Chen et al. (2018) also observed a higher increase of $\delta^{15}N\text{-}N_2O$ in microbial compared to abiotic NO_2^- reduction experiments. An alternative way to use the $\delta^{15}N\text{-}N_2O$ data to distinguish microbial and abiotic reactions could be modelling the substrate (NO_3^- or NO_2^-) and product (N_2O) $\delta^{15}N$ composition by applying the calculated $\varepsilon^{15}N_{NO3}$ and $\varepsilon^{15}N_{NO2}$ in batch experiments and to compare it with the determined $\delta^{15}N$ in the samples (Mariotti et al., 1981). Since N_2O is an intermediate product of the NO_3^- microbial reduction but the end product of the abiotic NO_2^- reduction, at the end of the reaction, the determined $\delta^{15}N\text{-}N_2O$ of the samples should fit the initial $\delta^{15}N$ of the substrate in the case of the NO_2^- abiotic reduction but should be higher than that in the case of the NO_3^- microbial reduction. For the microbial experiments with Mag-NP (BioSedGW-Mag-NP), the determined $\delta^{15}N\text{-}N_2O$ in most of the samples was above the modelled line, indicating a further reduction of the N_2O to N_2 (**Figure 6**). Contrarily, in the abiotic experiments with dissolved Fe^{2+} with or without micro-sized minerals ($AbFeNO_2$), the $\delta^{15}N\text{-}N_2O$ of the samples presented a tendency towards the substrate initial $\delta^{15}N$ at the end of the

reaction, confirming that N_2O was the end product of the NO_2^- abiotic reduction. The observation of some samples $\delta^{15}N\text{-}N_2O$ values below the modelled line, at the beginning of the reaction, suggested the generation of intermediate NO. Similar to our results, Chen et al. (2018) found initial $\delta^{15}N\text{-}N_2O$ more negative than the starting $\delta^{15}N\text{-}NO_3^-$ and $\delta^{15}N\text{-}NO_2^-$ due to NO generation. Also in another study, a good correlation was found between the calculated $\varepsilon^{15}N_{NO2}$ and the obtained $\delta^{15}N\text{-}N_2O$ values for the abiotic NO_2^- reduction by Fe(II) oxidation (Jones et al., 2015).

According to these results, the $\delta^{15}N\text{-}N_2O$ analysis is useful to determine if N_2O is an intermediate or final product of N compounds reduction. To quantify the contributions of microbial and abiotic NO_2^- reduction by Fe^{2+} oxidation, performing new experiments to determine the $\varepsilon^{15}N_{NO2}$ and the $\varepsilon^{15}N_{N2O}$ in microbial experiments could be advantageous after coupling this data to the already determined $\varepsilon^{15}N_{NO2}$ in abiotic experiments and $\varepsilon^{15}N_{NO3}$ in microbial experiments. Liu et al. (2018) assessed the contribution of each reaction by modelling the kinetics of each reaction tested separately. Concerning the Fe(II) oxidation, they found a major contribution of the abiotic compared to the microbial reaction while for the NO_2^- reduction, they found a major contribution of the microbial compared to the abiotic reaction. However, the use of models developed either by using isotopes or isotopic data could be limited at field-scale due to the complexity of the reactions. For example, Jamieson et al. (2018) suggested that the bacterial production of exopolymeric substances (EPS) could increase the NO_2^- abiotic reduction rate since Fe(II) can be complexed to the organic C from EPS. Other data that could be helpful in assessing the contribution of the microbial and abiotic reaction could be the analysis of the generated secondary minerals (Chen et al., 2018; Liu et al., 2018), the site preference (SP) of the generated N_2O (i.e. the intramolecular distribution of N isotopes since the N_2O molecule has an asymmetric linear structure (N-N-O)) (Buchwald et al., 2016; Heil et al., 2014; Jones et al., 2015) and the Fe(II) isotopic composition.

CONCLUSIONS

In our microbial experiments containing groundwater and sediment plus or without minerals (BioSedGW-Mag-NP/Mag/Sd/Ol/C), the beginning of denitrification was caused by heterotrophic bacteria that used organic C from sediment and/or groundwater. Afterwards, complete NO_3^- reduction to N_2 was only achieved in the BioSedGW-Mag-NP microcosms, suggesting an increased Fe(II) availability of nano-sized compared to micro-sized Mag. Reactivity between the Fe(II)-containing minerals and NO_3^- or NO_2^- was negligible. However, the abiotic NO_2^- reduction to N_2O by dissolved Fe^{2+} was demonstrated both in the presence and absence of micro-sized minerals (AbFeNO_2-Mag/Sd/Ol/C).

For the BioSedGW-Mag-NP experiments, the calculated $\varepsilon^{15}N_{NO3}$ was -33.1 ‰ (R^2 = 0.86), $\varepsilon^{18}O_{NO3}$ was -10.7 ‰ (R^2 = 0.74) and $\varepsilon^{15}N_{NO3}/\varepsilon^{18}O_{NO3}$ was 3.1, suggesting $\delta^{18}O$-NO_2^- equilibration with $\delta^{18}O$-H_2O and subsequent NO_2^- reoxidation to NO_3^-. The isotopic results for the BioSedGW-Mag/Ol/Sd experiments showed a similar trend since NPDOC released from sediment and groundwater was used as electron donor (uncomplete denitrification). Calculated $\varepsilon^{15}N_{NO3}$ was -12.0 ‰ (R^2 = 0.56), $\varepsilon^{18}O_{NO3}$ was -10.9 ‰ (R^2 = 0.63) and $\varepsilon^{15}N_{NO3}/\varepsilon^{18}O_{NO3}$ was 1.1, pointing to a lack of NO_2^- reoxidation. In the Ab$FeNO_2$ experiments, the $\varepsilon^{15}N_{NO2}$ ranged from -14.1 ‰ to -17.8 ‰ (R^2 > 0.89). Considering the wide range of $\varepsilon^{15}N_{NO2}$ values reported in the literature, it is not likely that the NO_2^- isotopic characterization can be useful at field-scale to distinguish homogeneous from heterogeneous reactions or abiotic from microbial NO_2^- reduction. Nevertheless, a high $\delta^{15}N$-N_2O enrichment with respect to the substrate could be indicative of microbial N compounds reduction. Also, modelling the $\delta^{15}N$-N_2O by applying the calculated $\varepsilon^{15}N_{NO3}$ and $\varepsilon^{15}N_{NO2}$ in batch experiments and comparing it with the determined isotopic composition in the samples can be used to confirm if N_2O is an

intermediate or final product of the reaction. Therefore, NO_2^- abiotic reaction by Fe(II) oxidation would be advantageous to avoid a water quality decrease due to NO_2^- accumulation in denitrification treatments only if the generated N_2O is further reduced to N_2 by microorganisms.

ACKNOWLEDGMENTS

This work has been financed by the following projects: NANOREMOV (CGL2017-87216-C4-3-R) and ISOTEC (CGL2017-87216-C4-1-R), financed by the Spanish Government and AEI/FEDER from the UE, and MAG (2017-SGR-1733) from the Catalan Government. Margalef-Marti, R. is grateful to the Spanish Government for the Ph.D. grant BES-2015-072882. We would like to thank the CCiT-UB for providing analytical support, Francesc Roca for his contribution on the Mag nanoparticles obtainment and Àngels Canals for her contribution on the XRD analysis and results interpretation.

REFERENCES

2006/118/EC, 2006. Groundwater Directive. Council Directive 2006/118/EC, of 12 December 2006, on the protection of groundwater against pollution and deterioration [WWW Document]. Off. J. Eur. Comm. URL http://ec.europa.eu/environment/index_en.htm (accessed 4.9.17).

91/676/EEC, 1991. Nitrates Directive. Council Directive 91/676/EEC of 12 December 1991, concerning the protection of waters against pollution caused by nitrates from agricultural sources. [WWW Document]. Off. J. Eur. Comm. URL http://ec.europa.eu/environment/index_en.htm (accessed 4.9.17).

98/83/EC, 1998. Drinking Water Directive. Council Directive 98/83/EC, of 3 November

1998, on the quality of water intended for human consumption. [WWW Document]. Off. J. Eur. Comm. URL http://ec.europa.eu/environment/index_en.htm (accessed 4.9.17).

Akunna, J.C., Bizeau, C., Moletta, R., 1993. Nitrate and nitrite reductions with anaerobic sludge using various carbon sources: Glucose, glycerol, acetic acid, lactic acid and methanol. Water Res. 27, 1303–1312. https://doi.org/10.1016/0043-1354(93)90217-6

Aquilina, L., Roques, C., Boisson, A., Vergnaud-Ayraud, V., Labasque, T., Pauwels, H., Pételet-Giraud, E., Pettenati, M., Dufresne, A., Bethencourt, L., Bour, O., 2018. Autotrophic denitrification supported by biotite dissolution in crystalline aquifers (1): New insights from short-term batch experiments. Sci. Total Environ. 619–620, 842–853. https://doi.org/10.1016/j.scitotenv.2017.11.079

Aravena, R., Robertson, W.D., 1998. Use of multiple isotope tracers to evaluate denitrification in ground water: study of nitrate from a large-flux septic system plume. Ground Water 36, 975–982.

Badr, O., Probert, S.D., 1993. Environmental impacts of atmospheric nitrous oxide. Appl. Energy 44, 197–231. https://doi.org/10.1016/0306-2619(93)90018-K

Betlach, M.R., Tiedje, J.M., 1981. Kinetic Explanation for Accumulation of Nitrite, Nitric Oxide, and Nitrous Oxide during Bacterial Denitrification. Appl. Environ. Microbiol. 42, 1074–1084. https://doi.org/Article

Bolleter, W.T., Bushman, C.J., Tidwell, P.W., 1961. Spectrophotometric Determination of Ammonia as Indophenol. Anal. Chem. 33, 592–594. https://doi.org/10.1021/ac60172a034

Borden, A.K., Brusseau, M.L., Carroll, K.C., McMillan, A., Akyol, N.H., Berkompas, J., Miao, Z., Jordan, F., Tick, G., Waugh, W.J., Glenn, E.P., 2012. Ethanol addition

for enhancing denitrification at the uranium mill tailing site in Monument Valley, AZ. Water. Air. Soil Pollut. 223, 755–763. https://doi.org/10.1007/s11270-011-0899-1

Bosch, J., Lee, K.Y., Jordan, G., Kim, K.W., Meckenstock, R.U., 2012. Anaerobic, nitrate-dependent oxidation of pyrite nanoparticles by *Thiobacillus denitrificans*. Environ. Sci. Technol. 46, 2095–2101. https://doi.org/10.1021/es2022329

Böttcher, J., Strebel, O., Voerkelius, S., Schmidt, H.-L., 1990. Using isotope fractionation of nitrate-nitrogen and nitrate-oxygen for evaluation of microbial denitrification in a sandy aquifer. J. Hydrol. 114, 413–424. https://doi.org/10.1016/0022-1694(90)90068-9

Braunschweig, J., Bosch, J., Meckenstock, R.U., 2013. Iron oxide nanoparticles in geomicrobiology: from biogeochemistry to bioremediation. N. Biotechnol. 30, 793–802. https://doi.org/10.1016/j.nbt.2013.03.008

Bryce, C., Blackwell, N., Schmidt, C., Otte, J., Huang, Y., Kleindienst, S., Tomaszewski, E., Schad, M., Warter, V., Peng, C., Byrne, J., Kappler, A., 2018. Microbial anaerobic Fe(II) oxidation - ecology, mechanisms and environmental implications. Environ. Microbiol. 20, 3462–3483. https://doi.org/10.1111/1462-2920.14328

Buchwald, C., Grabb, K., Hansel, C.M., Wankel, S.D., 2016. Constraining the role of iron in environmental nitrogen transformations: Dual stable isotope systematics of abiotic NO_2^- reduction by Fe(II) and its production of N_2O. Geochim. Cosmochim. Acta. https://doi.org/10.1016/j.gca.2016.04.041

Byrne, J.M., Dopffel, N., Rosso, K.M., Appel, E., 2015. Redox cycling of Fe(II) and Fe(III) in magnetite by Fe-metabolizing bacteria. https://doi.org/10.1126/science.aaa4834

Carlson, H.K., Clark, I.C., Blazewicz, S.J., Iavarone, A.T., Coates, J.D., 2013. Fe(II) oxidation is an innate capability of nitrate-reducing bacteria that involves abiotic and biotic reactions. J. Bacteriol. 195, 3260–3268. https://doi.org/10.1128/JB.00058-13

Carrey, R., Otero, N., Vidal-Gavilan, G., Ayora, C., Soler, A., Gómez-Alday, J.J., 2014. Induced nitrate attenuation by glucose in groundwater: Flow-through experiment. Chem. Geol. 370, 19–28. https://doi.org/10.1016/j.chemgeo.2014.01.016

Carrey, R., Rodríguez-Escales, P., Soler, A., Otero, N., 2018. Tracing the role of endogenous carbon in denitrification using wine industry by-product as an external electron donor: Coupling isotopic tools with mathematical modeling. J. Environ. Manage. 207, 105–115. https://doi.org/10.1016/j.jenvman.2017.10.063

Chen, D., Liu, T., Li, X., Li, F., Luo, X., Wu, Y., Wang, Y., 2018. Biological and chemical processes of microbially mediated nitrate-reducing Fe(II) oxidation by *Pseudogulbenkiania* sp. strain 2002. Chem. Geol. 476, 59–69. https://doi.org/10.1016/j.chemgeo.2017.11.004

Cho, D.W., Song, H., Kim, B., Schwartz, F.W., Jeon, B.H., 2015a. Reduction of nitrate in groundwater by Fe(0)/Magnetite nanoparticles entrapped in Ca-Alginate beads. Water. Air. Soil Pollut. 226. https://doi.org/10.1007/s11270-015-2467-6

Cho, D.W., Song, H., Schwartz, F.W., Kim, B., Jeon, B.H., 2015b. The role of magnetite nanoparticles in the reduction of nitrate in groundwater by zero-valent iron. Chemosphere 125, 41–49. https://doi.org/10.1016/j.chemosphere.2015.01.019

Chowdhury, S.R., Yanful, E.K., 2010. Arsenic and chromium removal by mixed magnetite-maghemite nanoparticles and the effect of phosphate on removal. J. Environ. Manage. 91, 2238–2247. https://doi.org/10.1016/j.jenvman.2010.06.003

Coby, A.J., Picardal, F.W., 2005. Inhibition of NO_3^- and NO_2- reduction by microbial Fe(III) reduction: Evidence of a reaction between NO_2^- and cell surface-bound Fe^{2+}. Appl. Environ. Microbiol. 71, 5267–5274. https://doi.org/10.1128/AEM.71.9.5267-5274.2005

Cooper, D.C., Picardal, F.W., Schimmelmann, A., Coby, A.J., 2003. Chemical and Biological Interactions during Nitrate and Goethite Reduction by *Shewanella putrefaciens* 200 Chemical and Biological Interactions during Nitrate and Goethite Reduction by Shewanella putrefaciens 200. Appl. Environ. Microbiol. 69, 3517–3525. https://doi.org/10.1128/AEM.69.6.3517

Coplen, T.B., 2011. Guidelines and recommended terms for expression of stable-isotope-ratio and gas-ratio measurement results. Rapid Commun. Mass Spectrom. 25, 2538–2560. https://doi.org/10.1002/rcm.5129

Crane, R.A., Dickinson, M., Popescu, I.C., Scott, T.B., 2011. Magnetite and zero-valent iron nanoparticles for the remediation of uranium contaminated environmental water. Water Res. 45, 2931–2942. https://doi.org/10.1016/j.watres.2011.03.012

Devlin, J.F., Eedy, R., Butler, B.J., 2000. The effects of electron donor and granular iron on nitrate transformation rates in sediments from a municipal water supply aquifer. J. Contam. Hydrol. 46, 81–97. https://doi.org/10.1016/S0169-7722(00)00126-1

Dhakal, P., Matocha, C.J., Huggins, F.E., Vandiviere, M.M., 2013. Nitrite reactivity with magnetite. Environ. Sci. Technol. 47, 6206–6213. https://doi.org/10.1021/es304011w

Fukada, T., Hiscock, K.M., Dennis, P.F., Grischek, T., 2003. A dual isotope approach to identify denitrification in groundwater at a river-bank infiltration site. Water Res. 37, 3070–3078. https://doi.org/10.1016/S0043-1354(03)00176-3

Ge, S., Peng, Y., Wang, S., Lu, C., Cao, X., Zhu, Y., 2012. Nitrite accumulation under constant temperature in anoxic denitrification process: The effects of carbon sources and COD/NO3-N. Bioresour. Technol. 114, 137–143. https://doi.org/10.1016/j.biortech.2012.03.016

Gibert, O., Pomierny, S., Rowe, I., Kalin, R.M., 2008. Selection of organic substrates as potential reactive materials for use in a denitrification permeable reactive barrier (PRB). Bioresour. Technol. 99, 7587–7596. https://doi.org/10.1016/j.biortech.2008.02.012

Gorski, C. a, Nurmi, J.T., Tratnyek, P.G., Hofstetter, T.B., Scherer, M.M., 2010. Redox Behavior of Magnetite : Reduction. Environ. Sci. Technol. 44, 55–60. https://doi.org/10.1021/es9016848

Grabb, K.C., Buchwald, C., Hansel, C.M., Wankel, S.D., 2017. A dual nitrite isotopic investigation of chemodenitrification by mineral-associated Fe(II) and its production of nitrous oxide. Geochim. Cosmochim. Acta 196, 388–402. https://doi.org/10.1016/j.gca.2016.10.026

Granger, J., Sigman, D.M., Lehmann, M.F., Tortell, P.D., 2008. Nitrogen and oxygen isotope fractionation during dissimilatory nitrate reduction by denitrifying bacteria. Limnol. Oceanogr. 53, 2533–2545. https://doi.org/10.4319/lo.2008.53.6.2533

Grau-Martínez, A., Torrentó, C., Carrey, R., Rodríguez-Escales, P., Domènech, C., Ghiglieri, G., Soler, A., Otero, N., 2017. Feasibility of two low-cost organic substrates for inducing denitrification in artificial recharge ponds: Batch and flow-through experiments. J. Contam. Hydrol. 198, 48–58. https://doi.org/10.1016/j.jconhyd.2017.01.001

He, S., Tominski, C., Kappler, A., Behrens, S., Roden, E.E., 2016. Metagenomic analyses of the autotrophic Fe(II)-oxidizing, nitrate-reducing enrichment culture

KS. Appl. Environ. Microbiol. 82, 2656–2668. https://doi.org/10.1128/AEM.03493-15

He, Y., Lin, H., Dong, Y., Li, B., Wang, L., Chu, S., Luo, M., Liu, J., 2018. Zeolite supported Fe/Ni bimetallic nanoparticles for simultaneous removal of nitrate and phosphate: Synergistic effect and mechanism. Chem. Eng. J. 347, 669–681. https://doi.org/10.1016/j.cej.2018.04.088

Heil, J., Wolf, B., Brüggemann, N., Emmenegger, L., Tuzson, B., Vereecken, H., Mohn, J., 2014. Site-specific ^{15}N isotopic signatures of abiotically produced N_2O. Geochim. Cosmochim. Acta 139, 72–82. https://doi.org/10.1016/j.gca.2014.04.037

Hernández-del Amo, E., Menció, A., Gich, F., Mas-Pla, J., Bañeras, L., 2018. Isotope and microbiome data provide complementary information to identify natural nitrate attenuation processes in groundwater. Sci. Total Environ. 613–614, 579–591. https://doi.org/10.1016/j.scitotenv.2017.09.018

Jamieson, J., Prommer, H., Kaksonen, A.H., Sun, J., Siade, A.J., Yusov, A., Bostick, B., 2018. Identifying and Quantifying the Intermediate Processes during Nitrate-Dependent Iron(II) Oxidation. Environ. Sci. Technol. 52, 5771–5781. https://doi.org/10.1021/acs.est.8b01122

Jones, L.C., Peters, B., Lezama Pacheco, J.S., Casciotti, K.L., Fendorf, S., 2015. Stable Isotopes and Iron Oxide Mineral Products as Markers of Chemodenitrification. Environ. Sci. Technol. 49, 3444–3452. https://doi.org/10.1021/es504862x

Jurado, A., Borges, A. V., Brouyère, S., 2017. Dynamics and emissions of N_2O in groundwater: A review. Sci. Total Environ. 584–585, 207–218. https://doi.org/10.1016/j.scitotenv.2017.01.127

Kampschreur, M.J., Kleerebezem, R., de Vet, W.W.J.M., Van Loosdrecht, M.C.M.,

2011. Reduced iron induced nitric oxide and nitrous oxide emission. Water Res. 45, 5945–5952. https://doi.org/10.1016/j.watres.2011.08.056

Klueglein, N., Kappler, A., 2013. Abiotic oxidation of Fe(II) by reactive nitrogen species in cultures of the nitrate-reducing Fe(II) oxidizer *Acidovorax* sp. BoFeN1 - questioning the existence of enzymatic Fe(II) oxidation. Geobiology 11, 180–190. https://doi.org/10.1111/gbi.12019

Knöller, K., Vogt, C., Haupt, M., Feisthauer, S., Richnow, H.H., 2011. Experimental investigation of nitrogen and oxygen isotope fractionation in nitrate and nitrite during denitrification. Biogeochemistry 103, 371–384. https://doi.org/10.1007/s10533-010-9483-9

Knowles, R., 1982. Denitrification. Microbiol. Rev. 46, 43–70.

Koch, H., Lücker, S., Albertsen, M., Kitzinger, K., Herbold, C., Spieck, E., 2015. Expanded metabolic versatility of ubiquitous nitrite-oxidizing bacteria from the genus *Nitrospira* 112, 11371–11376. https://doi.org/10.1073/pnas.1506533112

Liu, T., Chen, D., Luo, X., Li, X., Li, F., 2018. Microbially mediated nitrate-reducing Fe(II) oxidation: Quantification of chemodenitrification and biological reactions. Geochim. Cosmochim. Acta. https://doi.org/10.1016/j.gca.2018.06.040

Margalef-Marti, R., Carrey, R., Merchán, D., Soler, A., Causapé, J., Otero, N., 2019a. Feasibility of using rural waste products to increase the denitrification efficiency in a surface flow constructed wetland. J. Hydrol. 124035. https://doi.org/10.1016/j.jhydrol.2019.124035

Margalef-Marti, R., Carrey, R., Soler, A., Otero, N., 2019b. Evaluating the potential use of a dairy industry residue to induce denitri fi cation in polluted water bodies : A fl ow-through experiment. J. Environ. Manage. 245, 86–94. https://doi.org/10.1016/j.jenvman.2019.03.086

Margalef-Marti, R., Carrey, R., Viladés, M., Jubany, I., Vilanova, E., Grau, R., Soler, A., Otero, N., 2019c. Use of nitrogen and oxygen isotopes of dissolved nitrate to trace field-scale induced denitrification efficiency throughout an in-situ groundwater remediation strategy. Sci. Total Environ. https://doi.org/10.1016/j.scitotenv.2019.06.003

Mariotti, A., Germon, J.C., Hubert, P., Kaiser, P., Letolle, R., Tardieux, A., Tardieux, P., 1981. Experimental determination of nitrogen kinetic isotope fractionation: Some principles; illustration for the denitrification and nitrification processes. Plant Soil 62, 413–430. https://doi.org/10.1007/BF02374138

Mariotti, A., Landreau, A., Simon, B., 1988. ^{15}N isotope biogeochemistry and natural denitrification process in groundwater: Application to the chalk aquifer of northern France. Geochim. Cosmochim. Acta 52, 1869–1878. https://doi.org/10.1016/0016-7037(88)90010-5

Martin, T.S., Casciotti, K.L., 2016. Nitrogen and oxygen isotopic fractionation during microbial nitrite reduction. Limnol. Oceanogr. 61, 1134-1143. https://doi.org/ 10.1002/lno.10278

Matocha, C.J., Coyne, M.S., 2007. Short-term Response of Soil Iron to Nitrate Addition. Soil Sci. Soc. Am. J. 71, 108. https://doi.org/10.2136/sssaj2005.0170

McIlvin, M.R., Altabet, M.A., 2005. Chemical conversion of nitrate and nitrite to nitrous oxide for nitrogen and oxygen isotopic analysis in freshwater and seawater. Anal Chem 77, 5589–5595. https://doi.org/10.1021/ac050528s

Meckenstock, R.U., Morasch, B., Griebler, C., Richnow, H.H., 2004. Stable isotope fractionation analysis as a tool to monitor biodegradation in contaminated acquifers. J. Contam. Hydrol. 75, 215–255. https://doi.org/10.1016/j.jconhyd.2004.06.003

Melton, E.D., Swanner, E.D., Behrens, S., Schmidt, C., Kappler, A., 2014. The interplay of microbially mediated and abiotic reactions in the biogeochemical Fe cycle. Nat. Rev. Microbiol. 12, 797–808. https://doi.org/10.1038/nrmicro3347

Morley, N., Baggs, E.M., Dörsch, P., Bakken, L., 2008. Production of NO, N_2O and N_2 by extracted soil bacteria, regulation by NO_2^- and O_2 concentrations. FEMS Microbiol. Ecol. 65, 102–112. https://doi.org/10.1111/j.1574-6941.2008.00495.x

Otero, N., Torrentó, C., Soler, A., Menció, A., Mas-Pla, J., 2009. Monitoring groundwater nitrate attenuation in a regional system coupling hydrogeology with multi-isotopic methods: The case of Plana de Vic (Osona, Spain). Agric. Ecosyst. Environ. 133, 103–113. https://doi.org/10.1016/j.agee.2009.05.007

Pantke, C., Obst, M., Benzerara, K., Morin, G., Ona-nguema, G., Dippon, U., Kappler, A., 2012. Green Rust Formation during Fe(II) Oxidation by the Nitrate-Reducing *Acidovorax* sp. Strain BoFeN1. Environ. Sci. Technol. 1439–1446. https://doi.org/10.1021/es2016457

Price, A., Pearson, V.K., Schwenzer, S.P., Miot, J., Olsson-Francis, K., 2018. Nitrate-dependent iron oxidation: A potential Mars metabolism. Front. Microbiol. 9, 1–15. https://doi.org/10.3389/fmicb.2018.00513

Rakshit, S., Matocha, C.J., Coyne, M.S., Sarkar, D., 2016. Nitrite reduction by Fe(II) associated with kaolinite. Int. J. Environ. Sci. Technol. 13, 1329–1334. https://doi.org/10.1007/s13762-016-0971-x

Reay, D.S., Davidson, E.A., Smith, K.A., Smith, P., Melillo, J.M., Dentener, F., Crutzen, P.J., 2012. Global agriculture and nitrous oxide emissions. Nat. Clim. Chang. 2, 410–416. https://doi.org/10.1038/nclimate1458

Rivett, M.O., Buss, S.R., Morgan, P., Smith, J.W.N., Bemment, C.D., 2008. Nitrate attenuation in groundwater: A review of biogeochemical controlling processes.

Water Res. 42, 4215–4232. https://doi.org/10.1016/j.watres.2008.07.020

Ryabenko, E., Altabet, M. a., Wallace, D.W.R., 2009. Effect of chloride on the chemical conversion of nitrate to nitrous oxide for $\delta^{15}N$ analysis. Limnol. Oceanogr. Methods 7, 545–552. https://doi.org/10.4319/lom.2009.7.545

Si, Z., Song, X., Wang, Y., Cao, X., Zhao, Y., Wang, B., Chen, Y., Arefe, A., 2018. Intensified heterotrophic denitrification in constructed wetlands using four solid carbon sources: Denitrification efficiency and bacterial community structure. Bioresour. Technol. 267, 416–425. https://doi.org/10.1016/j.biortech.2018.07.029

Smith, R.L., Kent, D.B., Repert, D.A., Böhlke, J.K., 2017. Anoxic nitrate reduction coupled with iron oxidation and attenuation of dissolved arsenic and phosphate in a sand and gravel aquifer. Geochim. Cosmochim. Acta 196, 102–120. https://doi.org/10.1016/j.gca.2016.09.025

Smith, R.L., Miller, D.N., Brooks, M.H., Widdowson, M.A., Killingstad, M.W., 2001. In situ stimulation of groundwater denitrification with formate to remediate nitrate contamination. Environ. Sci. Technol. 35, 196–203. https://doi.org/10.1021/es001360p

Straub, K.L., Benz, M., Schink, B., Widdel, F., 1996. Anaerobic, nitrate-dependent microbial oxidation of ferrous iron. Appl. Environ. Microbiol. 62, 1458–1460. https://doi.org/

Tai, Y.L., Dempsey, B.A., 2009. Nitrite reduction with hydrous ferric oxide and Fe(II): Stoichiometry, rate, and mechanism. Water Res. 43, 546–552. https://doi.org/10.1016/j.watres.2008.10.055

Torrentó, C., Cama, J., Urmeneta, J., Otero, N., Soler, A., 2010. Denitrification of groundwater with pyrite and *Thiobacillus denitrificans*. Chem. Geol. 278, 80–91. https://doi.org/10.1016/j.chemgeo.2010.09.003

Torrentó, C., Urmeneta, J., Otero, N., Soler, A., Viñas, M., Cama, J., 2011. Enhanced denitrification in groundwater and sediments from a nitrate-contaminated aquifer after addition of pyrite. Chem. Geol. 287, 90–101. https://doi.org/10.1016/j.chemgeo.2011.06.002

Trois, C., Pisano, G., Oxarango, L., 2010. Alternative solutions for the bio-denitrification of landfill leachates using pine bark and compost. J. Hazard. Mater. 178, 1100–1105. https://doi.org/10.1016/j.jhazmat.2010.01.054

Tsushima, K., Ueda, S., Ohno, H., Ogura, N., Katase, T., Watanabe, K., 2006. Nitrate decrease with isotopic fractionation in riverside sediment column during infiltration experiment. Water. Air. Soil Pollut. 174, 47–61. https://doi.org/10.1007/s11270-005-9024-7

Vidal-Gavilan, G., Folch, A., Otero, N., Solanas, A.M., Soler, A., 2013. Isotope characterization of an in situ biodenitrification pilot-test in a fractured aquifer. Appl. Geochemistry 32, 153–163. https://doi.org/10.1016/j.apgeochem.2012.10.033

Vitòria, L., Soler, A., Canals, À., Otero, N., 2008. Environmental isotopes (N, S, C, O, D) to determine natural attenuation processes in nitrate contaminated waters: Example of Osona (NE Spain). Appl. Geochemistry 23, 3597–3611. https://doi.org/10.1016/j.apgeochem.2008.07.018

Vitousek, P.M., Aber, J.D., Howarth, R.W., Likens, G.E., Matson, P.A., Schindler, D.W., Schlesinger, W.H., Tilman, D.G., 1997. Summary for Policymakers, in: Intergovernmental Panel on Climate Change (Ed.), Climate Change 2013 - The Physical Science Basis. Cambridge University Press, Cambridge, pp. 1–30. https://doi.org/10.1017/CBO9781107415324.004

Wang, M., Hu, R., Zhao, J., Kuzyakov, Y., Liu, S., 2016. Iron oxidation affects nitrous oxide emissions via donating electrons to denitrification in paddy soils. Geoderma

271, 173–180. https://doi.org/10.1016/j.geoderma.2016.02.022

Ward, M.H., DeKok, T.M., Levallois, P., Brender, J., Gulis, G., Nolan, B.T., VanDerslice, J., 2005. Workgroup Report: Drinking-Water Nitrate and Health—Recent Findings and Research Needs. Environ. Health Perspect. 113, 1607–1614. https://doi.org/10.1289/ehp.8043

Weber, K.A., Achenbach, L.A., Coates, J.D., 2006. Microorganisms pumping iron: Anaerobic microbial iron oxidation and reduction. Nat. Rev. Microbiol. 4, 752–764. https://doi.org/10.1038/nrmicro1490

Weymann, D., Geistlinger, H., Well, R., Von Der Heide, C., Flessa, H., 2010. Kinetics of N_2O production and reduction in a nitrate-contaminated aquifer inferred from laboratory incubation experiments. Biogeosciences 7, 1953–1972. https://doi.org/10.5194/bg-7-1953-2010

Wunderlich, A., Meckenstock, R., Einsiedl, F., 2012. Effect of different carbon substrates on nitrate stable isotope fractionation during microbial denitrification. Environ. Sci. Technol. 46, 4861–4868. https://doi.org/10.1021/es204075b

Yan, R., Kappler, A., Muehe, E.M., Knorr, K.H., Horn, M.A., Poser, A., Lohmayer, R., Peiffer, S., 2019. Effect of Reduced Sulfur Species on Chemolithoautotrophic Pyrite Oxidation with Nitrate. Geomicrobiol. J. https://doi.org/10.1080/01490451.2018.1489915

Yang, Y., Chen, T., Morrison, L., Gerrity, S., Collins, G., Porca, E., Li, R., Zhan, X., 2017. Nanostructured pyrrhotite supports autotrophic denitrification for simultaneous nitrogen and phosphorus removal from secondary effluents. Chem. Eng. J. 328, 511–518. https://doi.org/10.1016/j.cej.2017.07.061

Zelmanov, G., Semiat, R., 2008. Iron(3) oxide-based nanoparticles as catalysts in advanced organic aqueous oxidation. Water Res. 42, 492–498.

https://doi.org/10.1016/j.watres.2007.07.045

Zhou, J., Wang, H., Yang, K., Ji, B., Chen, D., Zhang, H., Sun, Y., Tian, J., 2016. Autotrophic denitrification by nitrate-dependent Fe(II) oxidation in a continuous up-flow biofilter. Bioprocess Biosyst. Eng. 39, 277–284. https://doi.org/10.1007/s00449-015-1511-7

Zumft, W.G., 1997. Cell biology and molecular basis of denitrification. Microbiol. Mol. Biol. Rev. 61, 533–616.

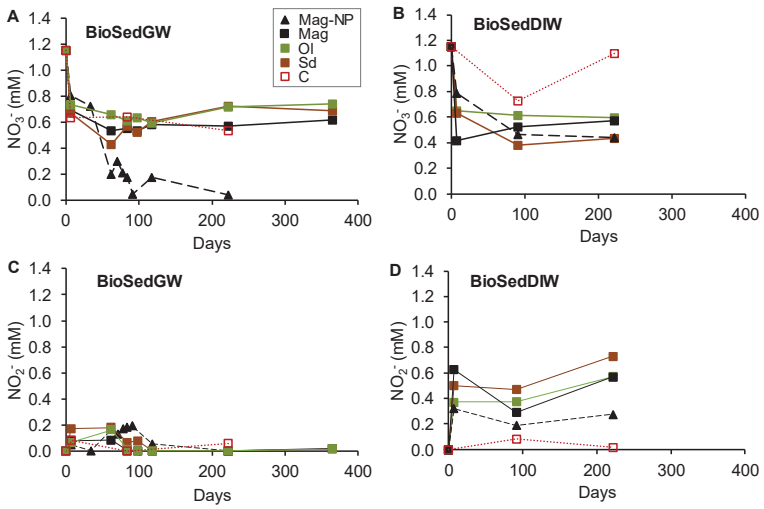

Figure 1. NO_3^- reduction in microbial experiments. NO_3^- (**A, B**) and NO_2^- (**C, D**) concentrations measured in the BioSedGW (**A, C**) and BioSedDIW (**B, D**) experiments, containing groundwater or deionized water, respectively. Both types of experiments contained sediment. In experiments labelled as Mag-NP, Mag, Sd, Ol minerals were added while in experiments labelled as C (control) no minerals were added.

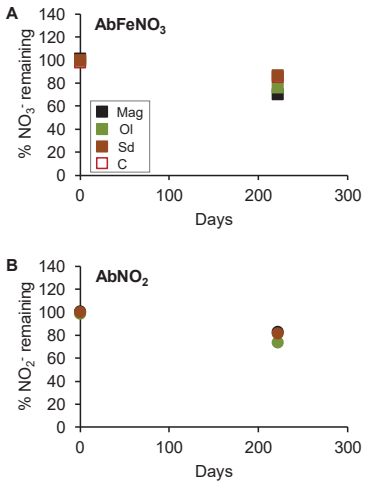

Figure 2. Lack of abiotic reactivity between NO_3^- and Fe(II) (dissolved or mineral) and between NO_2^- and the micro-sized minerals. Remaining NO_3^- (squares) or NO_2^- (circles) concentration in the $AbFeNO_3$ (**A**) and $AbNO_2$ (**B**) experiments, that contained deionized water with NO_3^- or NO_2^-, respectively. In experiments labelled as Mag-NP, Mag, Sd, Ol minerals were added while in experiments labelled as C (control) no minerals were added. Dissolved Fe^{2+} was added in the $AbFeNO_3$ experiments.

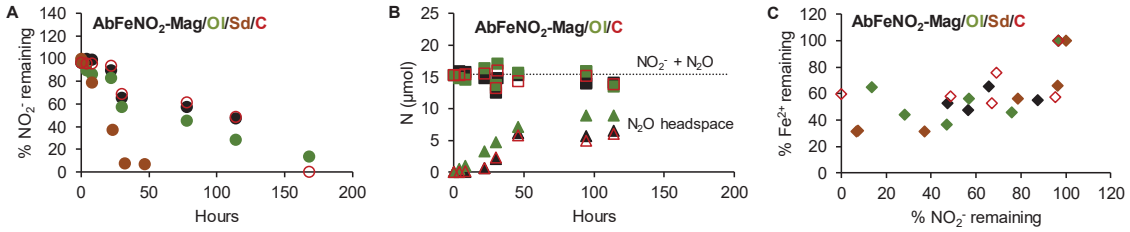

Figure 3. Abiotic reactivity between NO_2^- and dissolved Fe^{2+}. For the $AbFeNO_2$ experiments, (**A**) show the remaining NO_2^-. In (**B**), the accumulated N_2O is presented as triangles, the sum of accumulated N_2O and remaining NO_2^- is presented as squares and the dotted line reflects the NO_2^- initial content. (**C**) show the remaining dissolved Fe^{2+}. These experiments contained synthetic water with NO_2^- and dissolved Fe^{2+}. In experiments labelled as Mag, Sd or Ol, minerals were added while in experiments labelled as C (control), no minerals were added.

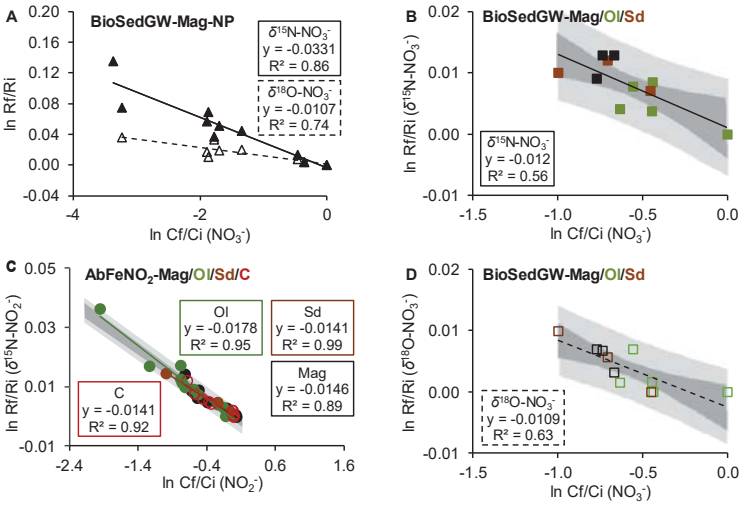

Figure 4. NO_3^- and NO_2^- ε calculation. (**A, B, D**) show the fractionation for the $\delta^{15}N\text{-}NO_3^-$ (continuous line) and $\delta^{18}O\text{-}NO_3^-$ (dotted line) in the microbial tests (BioSedGW-Mag-NP and BioSedGW-Mag/Ol/Sd/C, respectively). These experiments contained NO_3^- polluted groundwater and sediment plus minerals (Mag-NP, Mag, Ol, Sd). (**C**) show the $\delta^{15}N\text{-}NO_2^-$ fractionation in the abiotic tests ($AbFeNO_2$) containing synthetic water with NO_2^- and dissolved Fe^{2+} and involving the addition or lack of micro-sized minerals (Mag, Ol, Sd or C (control)). In the plots including different experiments, the shaded areas reflect the 95 % confidence interval.

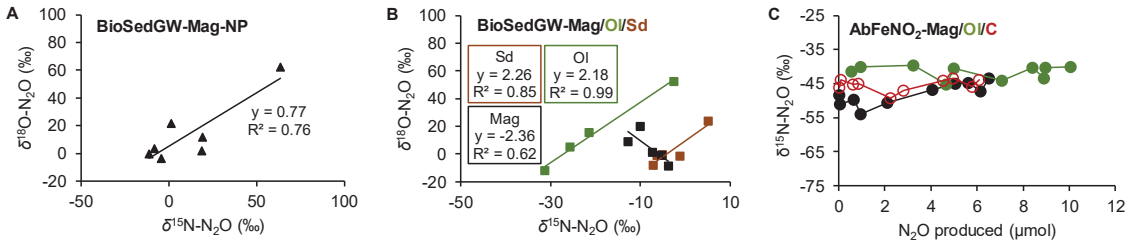

Figure 5. N_2O isotopic composition. $\delta^{15}N\text{-}N_2O$ versus $\delta^{18}O\text{-}N_2O$ plots for the microbial experiments BioSedGW-Mag-NP (**A**) and BioSedGW-Mag/Ol/Sd (**B**), which contained NO_3^- polluted groundwater and sediment plus minerals (Mag-NP or micro-sized Mag, Ol, Sd). For the abiotic tests ($AbFeNO_2$), which contained deionized water with NO_2^- and dissolved Fe^{2+} with or without addition of minerals (Mag, Ol or C (control)), the $\delta^{15}N\text{-}N_2O$ evolution along N_2O production is shown (**C**).

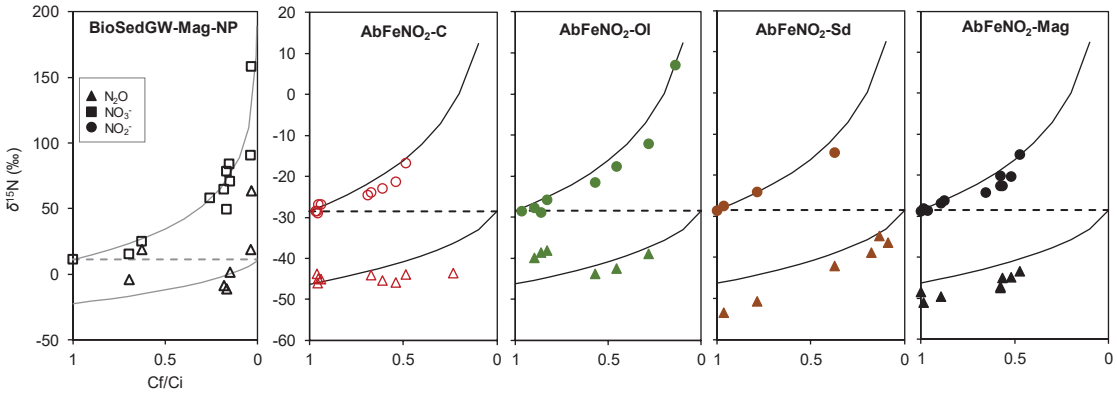

Figure 6. Modelled and measured $\delta^{15}N$ of the remaining substrate and generated N_2O. The BioSedGW-Mag-NP microcosms contained NO_3^- polluted groundwater and sediment plus Mag-NP (microbial). The $AbFeNO_2$ tests contained deionized water with NO_2^- and dissolved Fe^{2+} and involved the addition or lack of micro-sized minerals (Mag, Sd, Ol or C (control)) (abiotic). This model was first described by Mariotti et al. (1981) and was drawn using the ε values determined for the experiments.

Table 1. Microbial and abiotic experiments. Content of the batch experiments. N stands for the number of identical bottles. DIW refers to deionized water. (*) The number of bottles is for each mineral (Min) used (Mag, Ol, Sd, Mag-NP). C refers to the control without mineral.

Experiment	Conditions	N	Code
Microbial NO_3^- reduction (groundwater)	Sediment (2.5 g) + groundwater (15 mL, 1 mM NO_3^-)	3	BioSedGW-C
	Sediment (2.5 g) + groundwater (15 mL, 1 mM NO_3^-) + mineral (100 mg)	8 (*)	BioSedGW-Min
Microbial NO_3^- reduction (DIW)	Sediment (2.5 g) + DIW (15 mL, 1 mM NO_3^-)	3	BioSedDIW-C
	Sediment (2.5 g) + DIW (15 mL, 1 mM NO_3^-) + mineral (100 mg)	3 (*)	BioSedDIW-Min
Blank	Sediment (2.5 g) + MilliQ water (15 mL)	3	Blank
Abiotic NO_3^- reduction (synthetic water + Fe^{2+})	Synthetic water (10 mL, 1 mM NO_3^-) + $FeCl_2$ (5 mM)	3	Ab$FeNO_3$-C
	Synthetic water (10 mL, 1 mM NO_3^-) + $FeCl_2$ (5 mM) + mineral (50 mg)	3 (*)	Ab$FeNO_3$-Min
Abiotic NO_2^- reduction (synthetic water)	Synthetic water (10 mL, 1 mM NO_2^-) + mineral (50 mg)	3 (*)	AbNO_2-Min
Abiotic NO_2^- reduction (synthetic water + Fe^{2+})	Synthetic water (10 mL, 1 mM NO_2^-) + $FeCl_2$ (5 mM)	8	Ab$FeNO_2$-C
	Synthetic water (10 mL, 1 mM NO_2^-) + $FeCl_2$ (5 mM) + mineral (50 mg)	8 (*)	Ab$FeNO_2$-Min

Table 2. Range of $\varepsilon^{15}N$, $\varepsilon^{18}O$ and $\varepsilon^{15}N/\varepsilon^{18}O$ values reported in the literature for NO_3^- and NO_2^- reduction laboratory experiments. Both the microbial and abiotic reductions are included. For pure culture experiments, the enzymes are specified inside parentheses (if reported). n.d. = no determined.

ELECTRON ACCEPTOR	ELECTRON DONOR	INVOLVED MICROORGANISMS	$\varepsilon^{15}N$	$\varepsilon^{18}O$	$\varepsilon^{15}N/\varepsilon^{18}O$	REFERENCE
NO_3^-	C_{org}	*Ochrobactrum* sp., *Paracoccus denitrificans, Pseudomonas stutzeri* (NAR)	-5.4 to -26.6	-4.8 to -22.8	1.0 to 1.2	(Granger et al., 2008)
NO_3^-	C_{org}	*Rhodobacter sphaeroides* (NAP)	-16	-8.9	1.8	
NO_3^-	C_{org}	*Pseudomonas pseudoalcaligenes*, *Azoarcus* sp.	-8.6 to -16.2	-4.0 to -7.3	1.3 to 3.0	(Knöller et al., 2011)
NO_3^-	C_{org}	*Thauera aromatica, Aromatoleum aromaticum*	-17.3 to -23.5	-15.9 to -23.7	1.0 to 1.2	(Wunderlich et al., 2012)
NO_3^-	Compounds from riparian sediments and groundwater	Microorganisms from riparian sediments and groundwater	-32.9 to -34.1	n.d.	n.d.	(Tsushima et al., 2006)
NO_3^-	Pyrite	*Thiobacillus denitrificans*	-15.0 to -27.6	-13.5 to -21.3	1.1 to 1.3	(Torrentó et al., 2011, 2010)
NO_2^-	C_{org}	*Pseudomonas aeruginosa, Pseudomonas chlororaphis, Pseudomonas stutzeri* (Fe-NIR)	-3 to -11	-2 to -12	0.7 to 3.3	(Martin and Casciotti, 2016)
NO_2^-	C_{org}	*Achromobacter xylosoxidans, Ochrobactrum sp., Pseudomonas aureofaciens* (Cu-NIR)	-19 to -26	0 to -6	3.1 to 22.0	
NO_2^-	Nontronite	Abiotic	-11.1	-10.4	1.1	(Grabb et al., 2017)
NO_2^-	Aqueous + adsorbed Fe(II) (Nontronite)	Abiotic	-2.3	-4.5	0.5	
NO_2^-	Green rust	Abiotic	-4.2 to -9.4	-4.1 to -9.4	0.8 to 1.1	
NO_2^-	Aqueous Fe^{2+}	Abiotic	-6.1 to -33.9	-5.7 to -24.8	0.8 to 1.6	(Buchwald et al., 2016)
NO_2^-	Aqueous + adsorbed Fe(II) (Goethite)	Abiotic	-5.9 to -44.8	-5.2 to -33.0	1.0 to 1.4	
NO_2^-	Aqueous Fe^{2+}	Abiotic	-12.9	-9.8	1.3	(Jones et al., 2015)

Section S1. Micro-sized minerals preparation and magnetite size reduction

Magnetite (Mag) was obtained from “Mina Cala” (Huelva, Spain), siderite (Sd) from “El guarnón” (Güéjar Sierra, Granada, Spain) and olivine (Ol) from Canet d’Adri (Girona, Spain). The minerals were milled in a vibratory disc mill (RETSCH, RS 100) using a tungsten carbide bowl (WC 94%, Co 6%) and sieved to obtain the fraction with a particle size below 30 μm. An aliquot of Mag microparticles was then milled in a planetary ball mill (FRITSCH, PULVERISETTE P5) at 200 rpm during 15 h, using a stainless steel bowl, deionized water and 0.4 mm steel balls (S110) as grinding media to obtain nanoparticles.

Section S2. Mineral characterization

The main composition of the minerals was estimated by X-Ray Diffraction (XRD, PANalytical X'Pert PRO), the particle size of the Mag micro and nanoparticles was determined by Laser Diffraction Particle Size Analysis (LDPSA, LS13320, BeckmanCoulter) and morphology by Field Emission Scanning Electron Microscopy (FESEM, JSM-7610F, JEOL).

XRD analysis showed a purity of around 90% for Mag ($Fe(II)Fe(III)_2O_4$), 30% for Sd ($Fe(II)CO_3$) and 80% for Ol (Forsterite ferroan, $Fe(II)_{0.2}Mg_{1.8}SiO_4$). Therefore, the given Fe(II)/N molar ratio of the minerals in the microbial experiments was approximately 24 for Mag and Mag-NP, 13 for Sd and 7 for Ol. For Mag calculations, the Fe(II)/Fe(III) ratio was considered stoichiometric although it was not analyzed. In the abiotic experiments ($AbFeNO_3$ and $AbFeNO_2$), the ratio was reduced by half, but dissolved Fe^{2+} was added at a Fe^{2+}/N of 5. Therefore, although using the same quantity of mineral, in the experiments containing Mag and Mag-NP, the Fe(II) availability could be higher compared to Sd, and the Ol experiments could present the lowest electron donor availability. The stoichiometric Fe(II)/N reported for the NO_3^- and NO_2^- reductions are 5 and 2, respectively (**Equation S1** and **S2**) (Melton et al., 2014; Tai and Dempsey, 2009).

$$10Fe^{2+} + 2NO_3^- + 24H_2O \rightarrow 10Fe(OH)_3 + N_2 + 18H^+ \qquad \textbf{Equation S1}$$

$$4Fe^{2+} + 2NO_2^- + 5H_2O \rightarrow 4FeOOH + N_2O + 6H^+ \qquad \textbf{Equation S2}$$

According to the LDPSA analysis, the first milling and sieving step gave solid particles with an average Mag particle diameter of 8.12 µm (between 0.07 and 36.24 µm) and the second milling step gave aggregates with an average of 1.16 µm (between 0.04 and 2.00 µm) (Supplementary information, **Figure S1A**). The % volume mode was used for calculations. Although the particle diameter range was wide, a 10 fold decrease in the

mineral size was observed in the Mag-NP compared to the micro-sized Mag. Such decrease was confirmed by the FESEM images, where it was observed that Mag-NP aggregates are formed by smaller nanoparticles with an average particle diameter around 100 nm (Supplementary information, **Figure S1B**).

REFERENCES

Melton, E.D., Swanner, E.D., Behrens, S., Schmidt, C., Kappler, A., 2014. The interplay of microbially mediated and abiotic reactions in the biogeochemical Fe cycle. Nat. Rev. Microbiol. 12, 797–808. https://doi.org/10.1038/nrmicro3347

Tai, Y.L., Dempsey, B.A., 2009. Nitrite reduction with hydrous ferric oxide and Fe(II): Stoichiometry, rate, and mechanism. Water Res. 43, 546–552. https://doi.org/10.1016/j.watres.2008.10.055

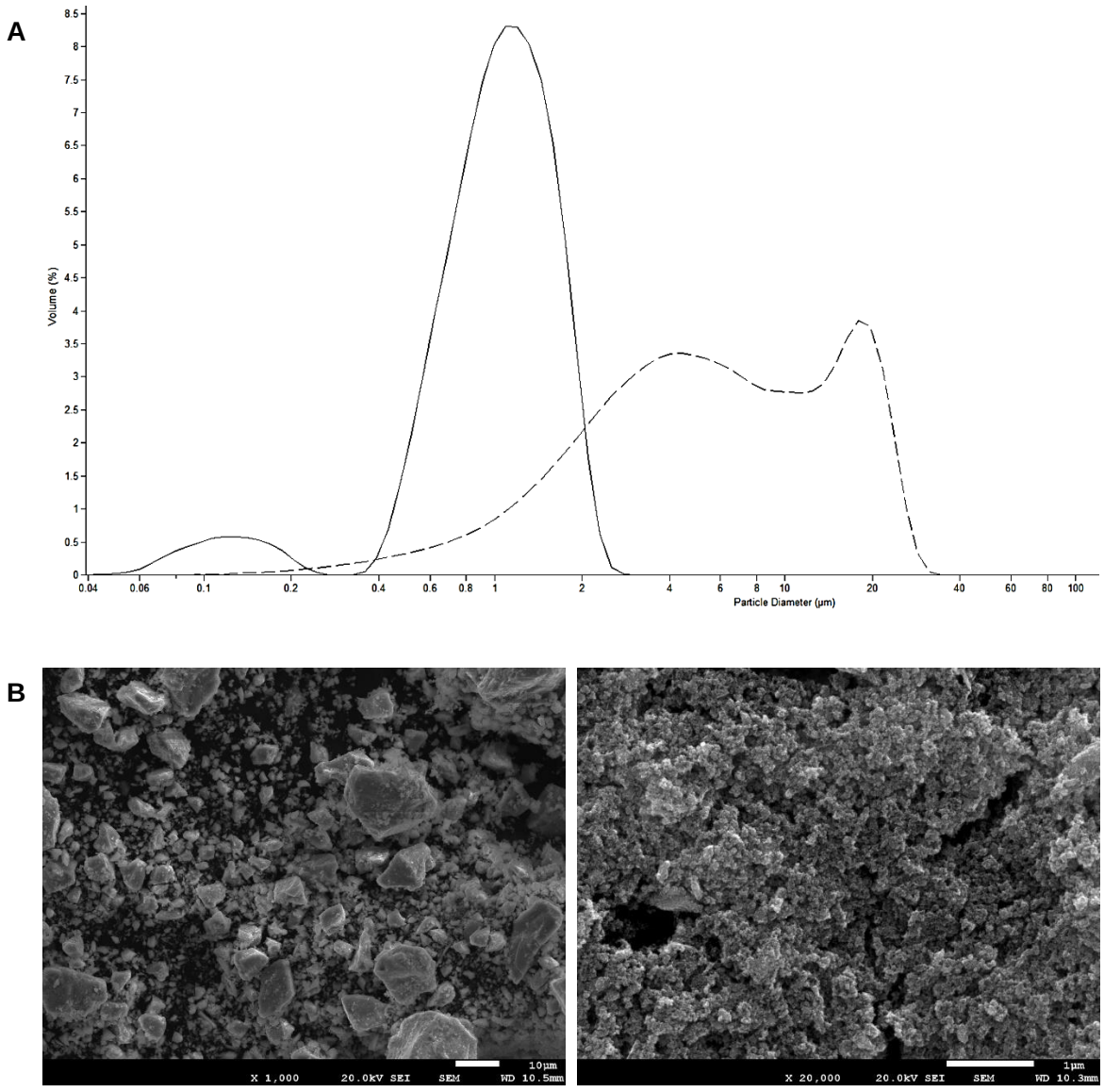

Figure S1. Mag particles characterization. A. Particle diameter before (dashed line) and after (continuous line) the second milling step. **B**. Particle morphology before (left) and after (right) the second milling step.

Table S1. Water composition for each series of experiments. Groundwater was used in the BioSedGW experiments, deionized water (DIW) in the BioSedDIW experiments and synthetic water (produced with DIW) in the $AbFeNO_3$, $AbFeNO_2$ and $AbNO_2$ experiments (see **Table 1**). Concentrations are expressed in ppm.

	BioSedGW	BioSedDIW	$AbFeNO_3$	$AbFeNO_2$ and $AbNO_2$
$NaHCO_3$	-	-	306.9	347.6
KH_2PO_4	-	-	4.9	7.0
$MgCl_2 \cdot 6H_2O$	-	-	259.9	275.6
KCl	-	-	107.3	116.0
$CaCl_2 \cdot 2H_2O$	-	-	124.8	99.3
Na_2SO_4	-	-	210.0	219.5
KNO_2	-	-	-	124.8
$NaNO_3$	-	97.7	0.104	-
Groundwater NO_3^-	71.3	-	-	-
Groundwater NPDOC	2.26	-	-	-

Table S2.1. Results for de BioSedGW experiments. Chemical and isotopic characterization. n.d. = non determined.

	Days	pH	NO_3^- (mM)	NO_2^- (mM)	NH_4^+ (mM)	N_2O (nmol)	$\delta^{15}N\text{-}NO_3^-$ (‰)	$\delta^{18}O\text{-}NO_3^-$ (‰)	$\delta^{15}N\text{-}N_2O$ (‰)	$\delta^{18}O\text{-}N_2O$ (‰)
Groundwater	0	7.6	1.15	0.00	n.d.	n.d.	+11.3	+10.1	n.d.	n.d.
BioSedGW-Mag-NP-1	7	5.8	0.80	0.05	0.00	7.1	+15.3	+14.3	-2.6	-41.2
BioSedGW-Mag-NP-2	34	n.d.	0.72	0.00	0.00	12.6	+24.8	+17.9	+20.4	-36.0
BioSedGW-Mag-NP-3	62	7.9	0.20	0.17	n.d.	0.9	+49.4	+44.0	-9.6	-37.7
BioSedGW-Mag-NP-4	71	7.1	0.30	0.13	n.d.	n.d.	+58.0	+30.2	n.d.	n.d.
BioSedGW-Mag-NP-5	78	7.1	0.21	0.17	0.00	38.2	+64.5	+29.8	-6.8	-33.9
BioSedGW-Mag-NP-6	84	7.2	0.17	0.18	n.d.	34.0	+71.0	+27.7	+2.9	-16.1
BioSedGW-Mag-NP-7	91	7.2	0.05	0.19	n.d.	43.3	+90.5	+47.5	+20.6	-26.1
BioSedGW-Mag-NP-8	118	7.1	0.18	0.05	0.00	0.0	+84.0	+20.9	n.d.	n.d.
BioSedGW-Mag-NP-9	222	7.0	0.04	0.00	0.03	63.8	+158.1	+25.0	+64.9	+24.9
BioSedGW-Ol-1	7	6.4	0.74	0.07	0.04	0.3	+15.1	+11.8	-29.8	-49.7
BioSedGW-Ol-2	62	8.1	0.66	0.16	0.04	0.6	+19.2	+17.1	n.d.	n.d.
BioSedGW-Ol-3	84	7.7	0.61	0.01	n.d.	0.6	+15.4	+11.6	-24.2	-32.8

Table S2.1. Continued.

	Days	pH	NO_3^- (mM)	NO_2^- (mM)	NH_4^+ (mM)	N_2O (nmol)	$\delta^{15}N\text{-}NO_3^-$ (‰)	$\delta^{18}O\text{-}NO_3^-$ (‰)	$\delta^{15}N\text{-}N_2O$ (‰)	$\delta^{18}O\text{-}N_2O$ (‰)
BioSedGW-Ol-4	98	7.6	0.63	0.00	0.02	0.36	n.d.	n.d.	-19.5	-22.0
BioSedGW-Ol-5	118	7.6	0.59	0.00	n.d.	0.00	n.d.	n.d.	n.d.	n.d.
BioSedGW-Ol-6	222	7.6	0.71	0.00	0.01	0.38	+19.9	+10.1	-1.2	+14.7
BioSedGW-Ol-7	365	n.d.	0.74	0.01	0.01	n.d.	n.d.	n.d.	n.d.	n.d.
BioSedGW-Sd-1	7	6.3	0.67	0.17	0.03	3.19	n.d.	n.d.	-4.9	-38.3
BioSedGW-Sd-2	62	7.6	0.43	0.18	0.04	7.43	+21.4	+20.2	-5.7	-46.0
BioSedGW-Sd-3	84	7.1	0.57	0.06	n.d.	11.06	+23.6	+15.8	-3.6	-38.0
BioSedGW-Sd-4	98	7.1	0.52	0.08	n.d.	14.19	n.d.	n.d.	+0.2	-39.0
BioSedGW-Sd-5	118	7.1	0.61	0.00	n.d.	0.00	n.d.	n.d.	n.d.	n.d.
BioSedGW-Sd-6	222	7.0	0.72	0.00	n.d.	6.55	+18.5	+10.1	+6.6	-13.5
BioSedGW-Sd-7	365	n.d.	0.69	0.02	0.01	n.d.	n.d.	n.d.	n.d.	n.d.
BioSedGW-Mag-1	7	6.3	0.69	0.08	0.04	2.42	n.d.	n.d.	-5.9	-36.5
BioSedGW-Mag-2	62	7.6	0.53	0.08	0.01	n.d.	+20.5	+17.1	n.d.	n.d.

Table S2.1. Continued.

	Days	pH	NO_3^- (mM)	NO_2^- (mM)	NH_4^+ (mM)	N_2O (nmol)	$\delta^{15}N\text{-}NO_3^-$ (‰)	$\delta^{18}O\text{-}NO_3^-$ (‰)	$\delta^{15}N\text{-}N_2O$ (‰)	$\delta^{18}O\text{-}N_2O$ (‰)
BioSedGW-Mag-3	84	7.2	0.55	0.00	n.d.	35.51	+24.4	+17.0	-2.3	-46.0
BioSedGW-Mag-4	98	7.2	0.53	0.00	0.00	0.94	n.d.	n.d.	-8.5	-17.4
BioSedGW-Mag-5	118	7.2	0.58	0.00	n.d.	3.16	n.d.	n.d.	-3.8	-38.3
BioSedGW-Mag-6	222	7.0	0.57	0.00	0.01	11.88	+24.4	+13.3	-11.3	-28.6
BioSedGW-Mag-7	365	n.d.	0.62	0.02	0.01	n.d.	n.d.	n.d.	n.d.	n.d.
BioSedGW-C-1	7	6.1	0.63	0.08	n.d.	6.87	+15.3	+13.7	-4.0	-42.0
BioSedGW-C-2	84	7.1	0.64	0.00	n.d.	0.00	n.d.	n.d.	n.d.	n.d.
BioSedGW-C-3	222	6.9	0.53	0.06	n.d.	n.d.	+29.2	+20.9	n.d.	n.d.

Table S2.2. ICP results for de BioSedGW-Mag-NP experiments. The results are expressed in ppm (semiquantitative). Pb, Cd, Co, Cu, Zn, Al, Be, Li, Mo, Ni, Sb, Ti, Tl, V, As, Cr, P, Se were also analyzed but concentrations were below detection limit. <d.l. = below detection limit. These results are not reported in the manuscript.

	Groundwater	BioSedGW-Mag-NP-1	BioSedGW-Mag-NP-2	BioSedGW-Mag-NP-4	BioSedGW-Mag-NP-5	BioSedGW-Mag-NP-6	BioSedGW-Mag-NP-7	BioSedGW-Mag-NP-8
Ca	92.73	113.63	116.47	98.91	108.03	102.82	100.53	96.00
Na	28.07	31.17	31.47	29.68	31.40	30.77	30.50	29.94
Mg	25.86	28.10	28.90	24.96	26.71	26.13	25.71	25.27
S	23.93	27.81	28.15	25.87	29.00	27.71	27.09	26.16
Si	13.70	5.56	4.64	4.70	4.59	4.54	4.67	4.15
K	5.04	5.80	4.91	4.84	10.21	12.61	5.88	6.02
B	2.85	2.72	2.75	2.97	2.86	3.36	3.13	2.97
Sr	1.13	0.72	0.67	0.64	0.66	0.64	0.63	0.60
Ba	0.05	< d.l.	<d.l.	0.01	<d.l.	<d.l.	0.01	<d.l.
Fe	0.02	0.04	0.03	0.02	0.02	0.03	0.03	0.01
Mn	0.00	0.15	0.15	0.06	0.07	0.07	0.06	0.06

Table S2.3. Results for de BioSedDIW experiments. Chemical and isotopic characterization. n.d. = non determined.

	Days	pH	NO_3^- (mM)	NO_2^- (mM)	NH_4^+ (mM)	N_2O (nmol)	$\delta^{15}N\text{-}NO_3^-$ (‰)	$\delta^{18}O\text{-}NO_3^-$ (‰)	$\delta^{15}N\text{-}N_2O$ (‰)	$\delta^{18}O\text{-}N_2O$ (‰)
DIW	0	n.d.	1.15	0.00	n.d.	n.d.	+16.9	+28.5	n.d.	n.d.
BioSedDIW-Ol-1	7	6.4	0.65	0.37	n.d.	0.12	+28.7	+43.9	-36.1	-48.3
BioSedDIW-Ol-2	91	8.9	0.61	0.38	n.d.	0.18	n.d.	n.d.	-15.7	-40.8
BioSedDIW-Ol-3	222	8.6	0.60	0.57	n.d.	n.d.	n.d.	n.d.	n.d.	n.d.
BioSedDIW-Sd-1	7	6.3	0.63	0.50	n.d.	0.24	n.d.	n.d.	-18.8	-44.2
BioSedDIW-Sd-2	91	7.8	0.38	0.47	n.d.	0.14	+24.2	+49.2	-12.8	-45.2
BioSedDIW-Sd-3	222	7.5	0.44	0.73	n.d.	n.d.	n.d.	n.d.	n.d.	n.d.
BioSedDIW-Mag-1	7	5.6	0.42	0.63	n.d.	0.11	n.d.	n.d.	-29.8	-46.3
BioSedDIW-Mag-2	91	8.1	0.52	0.29	n.d.	0.11	n.d.	n.d.	-18.5	-43.2
BioSedDIW-Mag-3	222	7.8	0.57	0.57	n.d.	n.d.	+15.1	+22.6	n.d.	n.d.
BioSedDIW-Mag-NP-1	7	5.8	0.79	0.32	n.d.	0.21	+20.5	+35.9	-28.5	-45.2
BioSedDIW-Mag-NP-2	91	7.8	0.46	0.19	n.d.	0.24	+29.8	+39.2	-10.3	-61.0
BioSedDIW-Mag-NP-3	222	7.6	0.44	0.28	n.d.	n.d.	n.d.	n.d.	n.d.	n.d.

Table S2.3. Continued.

	Days	pH	NO_3^- (mM)	NO_2^- (mM)	NH_4^+ (mM)	N_2O (nmol)	$\delta^{15}N\text{-}NO_3^-$ (‰)	$\delta^{18}O\text{-}NO_3^-$ (‰)	$\delta^{15}N\text{-}N_2O$ (‰)	$\delta^{18}O\text{-}N_2O$ (‰)
BioSedDIW-C-1	91	8.2	0.73	0.08	n.d.	0.00	n.d.	n.d.	n.d.	n.d.
BioSedDIW-C-2	222	n.d.	1.10	0.02	n.d.	n.d.	+16.34	+20.1	n.d.	n.d.

Table S2.4. Results for de AbFeNO3 experiments. Chemical and isotopic characterization. n.d. = non determined.

	Days	pH	NO_3^- (mM)	NO_2^- (mM)	N_2O (nmol)	$\delta^{15}N\text{-}NO_3^-$ (‰)	$\delta^{18}O\text{-}NO_3^-$ (‰)
Synthetic water	0	n.d.	1.48	0.00	n.d.	+16.9	+28.5
AbFeNO3-Mag-1	50	4.1	n.d.	n.d.	0.00	n.d.	n.d.
AbFeNO3-Mag-2	222	n.d.	1.04	0.02	n.d.	n.d.	n.d.
AbFeNO3-Ol-1	50	4.4	n.d.	n.d.	0.00	n.d.	n.d.
AbFeNO3-Ol-2	222	n.d.	1.12	0.01	n.d.	n.d.	n.d.
AbFeNO3-Sd-1	50	4	n.d.	n.d.	0.00	+16.7	+28.6
AbFeNO3-Sd-2	222	n.d.	1.28	0.01	n.d.	n.d.	n.d.
AbFeNO3-C-1	50	6.4	n.d.	n.d.	0.00	n.d.	n.d.
AbFeNO3-C-2	222	n.d.	1.26	0.01	n.d.	n.d.	n.d.

Table S2.5. Results for de AbNO2 experiments. Chemical characterization.

	Days	NO_3^- (mM)	NO_2^- (mM)
Synthetic water	0	0.00	1.52
AbNO2-Mag-1	222	0.01	1.26
AbNO2-Mag-2	365	0.01	1.38
AbNO2-Ol-1	222	0.00	1.13
AbNO2-Ol-2	365	0.02	1.23
AbNO2-Sd-1	222	0.01	1.24
AbNO2-Sd-2	365	0.11	1.11

Table S2.6. Results for de AbFeNO2 experiments. Chemical and isotopic characterization. n.d. = non determined.

	Hours	NO_2^- (mM)	NH_4^+ (mM)	$N\text{-}N_2O$ (µmol)	Fe (mM)	$\delta^{15}N\text{-}NO_2^-$ (‰)	$\delta^{18}O\text{-}NO_2^-$ (‰)
Synthetic water	0	1.10	n.d.	n.d.	5.00	-28.5	n.d.
AbFeNO2-Sd-1	2	1.06	0.0	n.d.	3.30	-27.4	-51.8
AbFeNO2-Sd-2	8	0.87	0.0	n.d.	2.81	-24.1	-49.2
AbFeNO2-Sd-3	23	0.41	0.0	n.d.	1.58	-14.5	-40.6
AbFeNO2-Sd-4	32	0.08	0.0	n.d.	1.60	n.d.	n.d.
AbFeNO2-Sd-5	47	0.07	0.0	n.d.	1.56	n.d.	n.d.
Synthetic water	0	1.54	n.d.	n.d.	5.00	-28.5	n.d.
AbFeNO2-Mag-1	4	1.59	n.d.	0.0	n.d.	-28.8	-46.9
AbFeNO2-Mag-2	8	1.57	n.d.	0.1	n.d.	-28.1	-49.5
AbFeNO2-Mag-3	22	1.42	n.d.	0.7	n.d.	-26.8	-48.1
AbFeNO2-Mag-4	30	1.04	n.d.	2.1	3.26	-24.2	-49.1
AbFeNO2-Mag-5	46	0.92	n.d.	6.2	n.d.	-20.1	-45.6
AbFeNO2-Mag-6	78	0.92	n.d.	n.d.	n.d.	-22.5	n.d.

Table S2.6. Continued.

	Hours	NO_2^- (mM)	NH_4^+ (mM)	$N\text{-}N_2O$ (µmol)	Fe (mM)	$\delta^{15}N\text{-}NO_2^-$ (‰)	$\delta^{18}O\text{-}NO_2^-$ (‰)
AbFeNO2-Mag-7	94	0.90	n.d.	5.1	2.38	-22.6	-43.4
AbFeNO2-Mag-8	114	0.75	n.d.	6.5	2.62	-14.9	-41.9
AbFeNO2-Ol-1	4	1.43	n.d.	0.6	n.d.	-27.7	-39.9
AbFeNO2-Ol-2	8	1.37	n.d.	1.0	n.d.	-28.8	-38.5
AbFeNO2-Ol-3	22	1.32	n.d.	3.3	n.d.	-25.8	-38.1
AbFeNO2-Ol-4	30	0.91	n.d.	4.7	2.80	-21.4	-43.7
AbFeNO2-Ol-5	46	0.86	n.d.	7.1	n.d.	-19.7	-42.7
AbFeNO2-Ol-6	78	0.72	n.d.	n.d.	n.d.	-17.6	-42.4
AbFeNO2-Ol-7	114	0.45	n.d.	9.0	2.20	-12.2	-38.9
AbFeNO2-Ol-8	168	0.22	n.d.	n.d.	3.23	7.1	n.d.

Table S2.6. Continued.

	Hours	NO_2^- (mM)	NH_4^+ (mM)	$N\text{-}N_2O$ (µmol)	Fe (mM)	$\delta^{15}N\text{-}NO_2^-$ (‰)	$\delta^{18}O\text{-}NO_2^-$ (‰)
AbFeNO2-C-1	4	1.52	n.d.	0.1	n.d.	-29.0	-44.6
AbFeNO2-C-2	8	1.53	n.d.	0.1	n.d.	-28.5	-42.3
AbFeNO2-C-3	22	1.49	n.d.	0.6	n.d.	-26.8	-43.6
AbFeNO2-C-4	30	1.10	n.d.	2.3	3.77	-24.5	-47.8
AbFeNO2-C-5	46	0.86	n.d.	5.8	n.d.	-21.3	-44.4
AbFeNO2-C-6	78	0.97	n.d.	n.d.	n.d.	-22.9	n.d.
AbFeNO2-C-7	114	0.78	n.d.	6.1	2.89	-16.8	-42.4
AbFeNO2-C-8	168	0.00	n.d.	n.d.	2.96	n.d.	n.d.

Table S2.7. ICP results for de AbFeNO2 experiments. The results are expressed in ppm (semiquantitative). Pb, Al, Be, Li, Mo, Sb, Ti, Tl, V, As, Cr and Se were also analyzed but concentrations were below detection limit. <d.l. = below detection limit; h = hours. The employed instrument for the analysis was: Perkin Elmer Optima 8300. These results are not reported in the manuscript.

	h	Ca	Mg	Ba	Cd	Co	Cu	Mn	Sr	Zn	K	Ni	Na	B	P	S	Si
AS	0	23.41	30.99	0.01	<d.l.	<d.l.	<d.l.	<d.l.	0.01	0.03	117.29	<d.l.	165.38	<d.l.	2.12	45.58	<d.l.
AbFeNO2-Sd-1	2	38.05	30.71	0.11	<d.l.	0.03	0.06	10.93	0.06	0.06	95.81	<d.l.	150.06	0.20	<d.l.	45.04	0.65
AbFeNO2-Sd-2	8	37.74	32.19	0.14	<d.l.	0.04	0.05	14.94	0.07	0.05	94.13	<d.l.	146.97	<d.l.	<d.l.	42.72	0.53
AbFeNO2-Sd-3	23	38.77	32.33	0.17	<d.l.	0.04	0.06	22.07	0.08	0.06	93.14	<d.l.	148.32	1.12	<d.l.	37.70	1.43
AbFeNO2-Sd-4	32	41.00	34.17	0.18	0.01	0.05	0.08	24.32	0.09	0.08	93.98	<d.l.	149.81	0.97	<d.l.	38.41	1.30
AbFeNO2-Sd-5	47	39.89	32.74	0.18	<d.l.	0.05	0.08	25.42	0.09	0.09	92.96	<d.l.	152.08	1.96	<d.l.	38.41	1.70
AbFeNO2-Mag-4	30	23.85	32.97	0.04	0.02	0.03	<d.l.	0.24	0.02	0.07	114.72	<d.l.	161.23	<d.l.	<d.l.	44.17	2.17
AbFeNO2-Mag-5	31	24.05	33.55	0.03	0.01	0.03	<d.l.	0.25	0.02	0.04	118.40	<d.l.	165.56	1.06	<d.l.	44.39	2.38
AbFeNO2-Mag-7	94	26.74	34.82	0.04	0.01	0.03	<d.l.	0.42	0.02	0.09	118.26	<d.l.	164.49	1.95	<d.l.	44.74	3.88
AbFeNO2-Mag-8	114	27.17	35.50	0.04	0.01	0.03	<d.l.	0.43	0.02	0.08	119.65	<d.l.	166.33	<d.l.	<d.l.	45.91	2.83
AbFeNO2-Ol-4	30	22.11	46.48	0.02	0.01	0.13	<d.l.	0.12	0.02	0.06	116.82	0.11	165.71	1.06	<d.l.	44.72	4.52
AbFeNO2-Ol-5	31	22.03	54.82	0.04	0.04	0.16	<d.l.	0.23	0.02	0.31	115.66	0.24	167.97	2.67	<d.l.	42.75	10.64
AbFeNO2-Ol-6	94	21.94	50.31	0.03	0.01	0.15	<d.l.	0.13	0.02	0.04	116.04	0.11	157.48	<d.l.	<d.l.	43.74	5.57
AbFeNO2-Ol-7	114	22.55	50.24	0.02	0.01	0.17	<d.l.	0.13	0.02	0.07	118.44	0.16	169.17	2.06	<d.l.	44.82	7.42
AbFeNO2-Ol-8	168	24.34	45.69	0.03	0.01	0.11	<d.l.	0.12	0.02	0.09	120.15	0.13	168.44	<d.l.	<d.l.	45.92	5.22

Table S2.7. Continued.

	h	Ca	Mg	Ba	Cd	Co	Cu	Mn	Sr	Zn	K	Ni	Na	B	P	S	Si
AbFeNO2-C-4	30	22.37	30.62	0.02	0.02	<d.l.	<d.l.	0.07	0.01	0.06	120.47	<d.l.	162.92	<d.l.	<d.l.	45.14	<d.l.
AbFeNO2-C-5	31	21.76	30.92	0.02	0.01	<d.l.	<d.l.	0.06	0.01	0.03	118.66	<d.l.	166.36	1.38	<d.l.	44.71	1.38
AbFeNO2-C-6	94	21.43	30.22	0.02	0.01	<d.l.	<d.l.	0.06	0.01	0.11	116.97	<d.l.	165.70	2.72	<d.l.	45.04	2.54
AbFeNO2-C-7	114	22.31	31.08	0.02	0.02	<d.l.	<d.l.	0.07	0.01	0.13	118.32	<d.l.	166.67	<d.l.	<d.l.	45.93	<d.l.
AbFeNO2-C-8	168	21.58	30.44	0.04	0.03	<d.l.	<d.l.	0.13	0.01	0.69	117.26	<d.l.	167.29	3.49	<d.l.	35.52	2.06

Table S2.8. Results of qualitative tests performed previously to the beginning of the present study. These batch experiments contained synthetic water with NO_3^- and micro-sized magnetite (bottles 1 to 4 contained 0.3 g, while bottles 5 to 8 contained 1.4 g). Set-up and incubation followed the same conditions than the abiotic experiments reported in **Table 1**. The qualitative concentration results were obtained by nitrate/nitrite test strips (Quantofix, Macherey-Nagel). In the table, for each bottle, the left column show nitrate and the right column nitrite concentrations (mg/L). Shaded cells reflect uncertainty in measurement.

Day/bottle	1		2		3		4		5		6		7		8	
0	100	0	100	0	100	0	100	0	100	0	100	0	100	0	100	0
6	100	0	100	0	100	0	100	0	100	0	100	0	100	0	100	0
14	100	0	100	0	100	0	100	0	100	0	100	0	100	0	100	0
22	100	0.5	100	0	100	0.5	100	0	100	0	100	0	100	0	100	0.5
32	100	0.5	100	0	100	0.5	100	0	100	0	100	0	100	0	100	0.5
42	100	0.5	100	0.5	100	0.5	100	0	100	0.5	100	0.5	100	0	100	0.5
49	100	0	100	0.5	100	0.5	100	0.5	100	0.5	100	0.5	100	0.5	100	0.5
56	100	0	100	0.5	100	0.5	100	0.5	100	0.5	100	0	100	0.5	100	0.5
63	100	0	75	0	100	0.5	100	0.5	-	-	100	0	100	0.5	100	0.5
69	-	-	75	0	100	0.5	100	0.5	-	-	100	0	100	0.5	100	0.5
76	-	-	75	0	100	0.5	100	0.5	-	-	100	0	100	0	100	0.5
86	-	-	100	0	100	0.5	100	0.5	-	-	100	0	100	0	100	0.5
104	-	-	100	0	100	0.5	100	0.5	-	-	100	0	100	0	100	0.5